CHANGES IN COCHLEAR FUNCTION AND SYNAPTIC PROTEIN EXPRESSION IN NOISE INDUCED COCHLEAR SYNAPTOPATHY

by

Kegan Ross Stephen

Submitted in partial fulfilment of the requirements
for the degree of Master of Science

at

Dalhousie University
Halifax, Nova Scotia
November 2017

Table of Contents

List of Tables

List of Figures

Abstract

As people age, the ability to understand fast speech and discern conversation in background noise becomes more difficult, despite normal audiological testing results. Perceptual difficulties in subjects with normal audiometric thresholds are referred to as hidden hearing loss (HHL), and are based on animal models that show noise can damage the delicate ribbon synapses between inner hair cells (IHCs) and spiral ganglion neurons (SGNs) without causing a permanent threshold shift (PTS). The issue of whether or not damage to the ribbon synapses can be reversed has been controversial. Therefore, the focus of this project was to verify molecular changes that may serve as further evidence of synaptic repair. Using Western Blotting to analyze proteins and Reverse Transcription quantitative Polymerase Chain Reaction (RT-qPCR) for messenger ribonucleic acid (mRNA) analysis, several proteins of the ribbon synapse were studied at several time points after noise exposure in a guinea pig model. In addition, other members in our lab evaluated how the cochlear responses (using compound action potential, CAP) from signals with large dynamic level changes (by utilizing amplitude modulation, AM) at a relatively high sound level (80 dB SPL) was impaired with noise induced hidden hearing loss (NIHHL). The number of synapses were also counted by other members in the lab to confirm the consistency of the model used in this project as compared with that found in previous studies.

There is a trend of up-regulation in the expression of ribbon protein at the RNA level one week post-noise exposure. This could suggest a synaptic repair, following the timeline previously found in guinea pigs after NIHHL (Song et al., 2016). However, the RNA level of GAP43, a critical protein for synaptic formation and plasticity, was found down-regulated in this thesis study, which could oppose prior findings of up-regulation of the protein itself (Dodson & Mohuiddin, 2000). Additionally, concern about the use of reference genes was raised and discussed in this thesis for the RNA analysis.

Morphologically, the synapse counts per IHC (synapse density) were similar to what was reported in guinea pigs as evaluated one month after the noise exposure: there was a significant reduction in synapses at the high-frequency region (between 8-32 kHz). Responses of the compound action potential (CAP) at high modulation frequencies (~1 kHz) to signals with dynamic amplitude changes remained highly depressed one month after the noise exposure. The reduction of the AM CAP amplitude appeared to be larger than the reduction of the synapse count. This is consistent with the idea that the noise exposure selectively damages the synapses innervating a special group of auditory nerve fibers that are important for the coding of signals with a larger dynamic range at high sound level. The results of this study further suggest that the repaired synapses are functionally abnormal.

List of Abbreviations and Symbols Used

µg	Micrograms
µL	Microlitres
µV	microvolts
× g	G-force
%	Percent (*w/v*)
AM	Amplitude modulation/modulated
ABR	Auditory Brainstem Response
ANF	Auditory nerve fibers
Bsn	Bassoon
B2m	Beta-2-microglobulin
CM	Cochlear microphonics
CAP	Compound action potential
Ctrl	Control
Ctbp2	C-terminal binding protein 2
dB	Decibels
DPN	Day post-noise
EFR	Envelope following response
EDTA	Ethylenediaminetetraacetic acid
FSL	First spike latency
g/L	Grams per litre

GAP43	Growth associated protein 43
HHL	Hidden hearing loss
Hprt1	Hypoxanthine phosphoribosyltransferase 1
IHCs	Inner hair cells
I/O	Input/output
ICI	Inter-click-interval
kDA	Kilodaltons
L	Litres
mRNA	Messenger ribonucleic acid
mL	Millilitres
mM	Millimolar
MF	Modulation/modulated frequency
M	Molar
MPN	Month post-noise
Nm	Nanometers
NCBI	National Center of Biotechnology Information
NIHL	Noise induced hearing loss
NIHHL	Noise induced hidden hearing loss
NRT	No-reverse transcriptase control
NTC	No-template control
OAEs	Otoacoustic emissions
PAGE	Polyacrylamide gel electrophoresis

PVDF	Polyvinylidene fluoride
PTS	Permanent threshold shift
RRP	Readily releasable pool
Rim2	Regulating synaptic membrane exocytosis 2
Rplp0	Ribosomal protein, large, P0
SRP	Slow releasable pool
SDS-PAGE	sodium dodecyl sulfate-polyacryamide gel electrophoresis
SPL	Sound pressure level
SGN	Spiral ganglion neuron
SD	Standard deviation
SEM	Standard error of the mean
Tbp	TATA box binding protein
TTS	Temporary threshold shift
TBS-T	Tris buffered saline with Tween-20
Tris	tris(hydroxymethyl)aminomethane
V	Volts
WPN	Week post-noise

Acknowledgements

I would like to thank my supervisor, Dr. Jian Wang, for his guidance in both the research and the writing of the report. The use of both Dr. George Robertson's lab and Dr. Paola Marcato's lab in undertaking this thesis was extremely fortuitous and without access the research could not have been completed. I would like to thank the Canadian Institutes of Health Research (CIHR) for the scholarship I received during my program. A big thank you also goes to Zhiping Yu, Hengchao Chen, Elizabeth Belland and Matthew Nichols, for assistance in instrumentation, usage, and access to their experience concerning various protocols. Hengchao Chen was a big contributor to the research as he collected and analyzed the electrophysiological data. Zhiping Yu conducted and analyzed experiments with regards to the synaptic counts. A big thank you to my committee, Drs. Steve Aiken and Michael Kiefte for their feedback. I would like to acknowledge Peter Cahill, Lisa Beck, Eleanor Campbell, Bonita Squires, Emily McGuire, Jennika Soles and Sarah Martin, for their very helpful suggestions for the development of this project. Guidance with regards to the administration work that comes with a thesis was given by Mark Monk, Crystal Vaughan and Joanne Fenerty. Finally, I appreciate all the support received from my family, with a special thank you to Justin Watts.

Chapter 1 Introduction

1.1 Noise Exposure and Permanent Threshold Shifts

Approximately 40% of Canadians aged 20 to 79 have at least some form of hearing loss, as indicated by elevated audiometric thresholds (Statistics Canada, 2016). The causes of this condition include, but are not limited to, aging (presbycusis), genetics, and noise exposure. Age and an accumulation of noise exposure can increase in tandem, and this exposure can cause peripheral auditory damage. Noise induced hearing loss (NIHL) is understood to be the only known preventable type of hearing loss (Neitzel, Swinburn, Hammer, & Eisenberg, 2016; Shaw, 2017). Overall, NIHL has been estimated to impact 25% of the United States population with a diagnosable hearing loss (Neitzel et al., 2016).

NIHL is typically quantified by the elevation of an individual's hearing thresholds. A higher level of noise and a longer duration of exposure will typically result in an increase in the amount of threshold elevation recorded (Health Canada, 2016). The threshold shift is usually largest when tested immediately after the exposure to continuous noise. This threshold shift can be partially recovered and therefore it is called a temporary threshold shift (TTS) (Kramer, Jerger & Mueller, 2014, p. 285-286). Depending on the dosage of noise exposure, considering both sound intensity and duration, the threshold shift may not totally recover and therefore results in what is called a permanent threshold shift (PTS). PTS is related to permanent damage to the auditory system due to noise exposure. Consequently, safety standards have been established based upon whether there is a potential for PTS or not.

Those who express concerns regarding their ability to hear do not always test poorly with traditional audiogram testing. This false negative is because the traditional audiogram will only detect their hearing sensitivity threshold at the level of the peripheral auditory system (Bharadwaj, Masud, Mehraei, Verhulst, & Shinn-Cunningham, 2015; Hind et al., 2011; Plack, Barker, & Prendergast, 2014). Regardless, even with (near) normal hearing thresholds, they still report difficulties with following fast signal changes and with perceiving speech in background noise (Hind et al., 2011; Plack et al., 2014). One study looked at typical caseloads in the United Kingdom and found that in their adult patients under sixty years of age, 5% of those who presented with these concerns had thresholds within normal limits (Hind et al., 2011). This minority of the caseload presents an interesting challenge to the way hearing loss has been traditionally defined. These cases demonstrate that there exist hearing impairments that the standard audiogram is unable to detect, and that the current model of diagnosing hearing loss and prescribing amplification is insufficient. The mechanisms of the hearing difficulties for these patients can be conceptualized by the newly defined phenomenon of hidden hearing loss (HHL), which is a consequence of noise exposure and noise induced hidden hearing loss (NIHHL) due to noise induced damage to cochlear afferent synapses without PTS. NIHHL is the focus of this thesis, as it remains a new and understudied phenomenon.

1.2 Noise Induced Hidden Hearing Loss and its Auditory Consequences

NIHHL was originally discovered in mice (Kujawa & Liberman, 2009). It was found that exposure to noise that only causes temporary threshold shifts (TTS) damaged the synapses between IHCs and type I spiral ganglion neurons (SGN), resulting in a

slowly developed degenerative death of the SGNs. The IHCs provide the means for sound to be transduced from mechanical energy to an electrical potential response (Gelfand, 2010, p. 37). In contrast, the temporary threshold shifts were also associated with recovered outer hair cell (OHC) responses, detected via otoacoustic emissions. This suggests that under such noise exposure, OHCs were not permanently damaged.

Interestingly, the recovery of thresholds gives the false idea that the recovery for the auditory system is complete, but the neural and synaptic degradation suggests damage is permanent - at least after two months post-noise exposure (Kujawa & Liberman, 2009). This damage and the functional deficits are referred to as cochlear synaptopathy. The discovery of NIHHL is significant because it suggests that PTS is a poor measure on which to base noise exposure guidelines.

The next question to answer is: what functional limitations exist for a cochlea in a subject with synaptic damage but not a PTS? Based upon available data, the limitations may present in several ways. Firstly, the massive damage to the synapses results in a greater portion of the auditory nerve fibers (ANFs) becoming idle, which may deteriorate the ability of ANFs to encode complex stimuli or the fine details of incoming auditory signals. In addition, the damaged synapses innervate a select group of ANFs that have a special functional role in signal coding at high sound level and with high background noise. As a consequence of the damage, the ANFs are unable to perform this crucial role, thus resulting in the reported difficulties with understanding speech in background noise. Finally, the repaired synapses may be functionally abnormal and the surviving synapses may not function normally.

The reduced cochlear output from ANFs has been functionally detected by various means in subjects with NIHHL. For example, the amplitude of the auditory brainstem response (ABR) wave I has been found to be permanently decreased after NIHHL noise exposure in animals (Kujawa & Liberman, 2009; Lobarinas, Spankovich, & Le Prell, 2016). A significant reduction in the amplitude of the compound action potential (CAP) has also been reported (Liu et al., 2012; Shi et al., 2013; Song et al., 2016). Studies in humans have similarly shown a reduced wave I ABR in young veterans with previous noise exposure without permanent threshold shifts that would indicate a typically defined hearing loss (Bramhall, Konrad-Martin, McMillan, & Griest, 2017). It is noteworthy that wave I of the human ABR is not as robust as in laboratory animals; however, the CAP can be recorded more reliably from the human external auditory canal (Liberman, Epstein, Cleveland, Wang, & Maison, 2016). In fact, the CAP has been recorded in humans together with the summating potential (SP) and the change in the SP/CAP amplitude ratio has been used to quantify cochlear synaptopathy. This ratio has been found to be increased for people with higher amounts of noise exposure, which also suggests a reduction of cochlear output. To understand these neural responses, the important junction of the synapse between IHCs and the ANFs has been investigated previously.

1.3 Low Spontaneous Nerve Fibres and NIHHL

Type I SGNs and ANFs are categorized based upon their spontaneous spike rate (SR), which is inversely associated with their threshold and dynamic range. Interestingly, each afferent neuron, referred to as SGN type I, synapses with only one IHC (Moser, Brandt, & Lysakowski, 2006), but each IHC is innervated by 5-30 SGNs

with synapses surrounding the bottom of the cell body. Based upon limited data obtained with a tracing technique, it is assumed the ANFs innervating IHCs towards the modiolar side of IHCs have lower-SRs, higher thresholds and a larger dynamic range (Heil & Peterson, 2015; Liberman, 1982; Moser et al., 2006). More recently, an immunohistology study on synaptic structure shows that the synapses located towards the modiolar side (the medial side) have relatively larger presynaptic ribbons and small post-synaptic terminals; whereas the synapses located towards the pillar side (the lateral side) have smaller ribbons and larger post-synaptic terminals (Liberman, Wang, & Liberman, 2011; Merchan-Perez & Liberman, 1996; Moser et al., 2006). Such morphological difference is likely the basis for the above categorization of ANFs. While the high-SR ANFs have low thresholds and are responsible for auditory sensitivity, they generally have a smaller dynamic range in intensity coding because their response to sound is quickly saturated with increasing sound level. It is interesting to note that low-SR nerves are conceptualized to increase the dynamic range of hearing and to reduce masking within background noise by still being available to fire when high spontaneous nerves with low thresholds have been exhausted or busy (Furman, Kujawa, & Liberman, 2013).

As a potential mechanism for the hearing deficits seen in NIHHL, it has been found that synapses to low-SR ANFs are more sensitive to noise damage and are the major category of ANFs that lose function after a noise exposure without PTS (Furman et al., 2013). Theoretically, the selective loss of this group of ANFs would result in coding deficits at high sound levels and/or in noisy backgrounds. However, in this study with Furman's group, no coding deficits (using ABR and tuning thresholds at the single unit level) were documented other than the loss of low-SR units.

There is no evidence at the single unit level of how ANFs change their coding in background noise and to signals with large dynamic ranges in noise induced synaptic damage that occurs more to the lower-SR units. Since amplitude modulation can provide a big change in signal amplitude, it is likely to be used for the evaluation of coding deficits to dynamic signals associated with the loss and unhealthy repair of low-SR ANFs. The envelope following responses (EFRs) to AM have been investigated in far-field recording and the impact of NIHHL on EFRs has been documented (Plack et al., 2014). In this thesis, the AM CAP was recorded by others currently in Dr. Wang's lab to further verify the change of cochlear function after noise-induced damage to the ribbon synapses.

1.4 Presynaptic Ribbon Selectively Damaged by Noise Exposure

The IHC-SGN synapse in the mammalian cochlea is characterized by a ribbon-like bend in the presynaptic region and called the ribbon synapse. The ribbon synapse is not unique to auditory hair cells, but is also present for other sensory encoding pathways such as vestibular hair cells, vertebrate photoreceptor cells, and bipolar cells of the retina (Sterling & Matthews, 2005). These electron-dense protein complexes are understood to be important with regards to recycling neurotransmitters to ensure continuous responses to afferent neurons from graded potential changes (Safieddine, El-Amraoui, & Petit, 2012; Sterling & Matthews, 2005). However, even though a pre-synaptic ribbon is present in varying cell types with a similar function, differences do exist. Retinal ribbon complexes are much more abundant, and subsequently easier to detect, than those in hair cells (Uthaiah & Hudspeth, 2010). Additionally, the retinal ribbon is more plate-shaped, where the hair cell ribbon is more spherical (Sterling & Matthews, 2005). Both ribbon

complexes appear to use glutamate as the neurotransmitter of choice. With regards to auditory functioning, sound encoding by afferent neurons plays a big role with IHCs (Safieddine et al., 2012), which will be the focus of this study.

A special role of the presynaptic ribbons in the auditory sensory cells (IHCs) is to facilitate the neurotransmitter release responsible for the high temporal resolution of signal transmission across these synapses (Safieddine, El-Amraoui, & Petit, 2012). This is very important for auditory functioning, because unlike other sensory organs (e.g., the retina), the auditory system relies heavily upon its temporal processing ability (Gelfand, 2010, p. 175-177). The ribbon complex has both tethered and docked vesicles filled with neurotransmitters (Safieddine et al., 2012). The docked vesicles refer to the compliment that reside beneath the ribbon next to the plasma membrane. The docked vesicles have been determined to be a readily releasable pool (RRP) for quick graded potential changes, whereas the tethered vesicles are a slow releasable pool (SRP) for prolonged sound exposure (Khimich et al., 2005; Moser et al., 2006; Safieddine et al., 2012). Current theory suggests that these pools of neurotransmitters are organized by the ribbon complex with regards to synchronous multi-vesicle release during prolonged sound exposure, but also for other temporal auditory processing (Glowatzki & Fuchs, 2002; Khimich et al., 2005).

Theoretically, noise induced synaptopathy should also impact the temporal processing ability of the cochlea. The evidence for temporal processing deficits have been obtained in animal studies. Such difficulties were seen in animals one month post-noise exposure when examined with a paired-click paradigm with differing inter-click intervals (ICI) at the brainstem level with auditory brainstem responses (ABRs) (Liu et

al., 2012), at the cochlear level with compound action potentials (CAPs) (Shi et al., 2013) and at the single unit SGN level with various measures (Song et al., 2016). In humans, associations with smaller latency of off-frequency masking of wave V of the ABR has been made with reduced ability to localize sound using an inter-aural time differences task (Mehraei et al., 2016). All of these results indicate temporal processing difficulties.

Such difficulties could present themselves as the previously mentioned symptom of trouble understanding speech with background noise. For example, a study using an acoustic cuing response at a low signal-to-noise ratio has resulted in poorer adaptive behaviour to the associated air puff for rats with NIHHL when compared to controls (Lobarinas et al., 2016). In other words, rats with NIHHL respond less to specific sounds when noise is introduced. That study makes a comparison between those rats and humans with listening to speech signals in challenging environments.

1.5 Presynaptic Ribbon Repair Controversy

Currently, there is a debate about whether the massive noise-induced damage to IHC-SGN synapses can be repaired. Studies reported by Liberman's group using CBA mice suggested that the damage was virtually unrepairable (Kujawa & Liberman, 2009). However, other studies show that the initially damaged synapses can be mostly, although not completely, repaired (Liu et al., 2012; Shi et al., 2013; Song et al., 2016). This was evident in the recovery of the synapse counts in immunohistology, and the significant recovery of CAP amplitudes after their initial depression (Liu et al., 2012; Shi et al., 2013; Song et al., 2016). More importantly, functional deficits were developed in association with recovery, suggesting that the repaired synapses were not healthy. To reiterate what was stated previously, temporal processing difficulties were present one

month post-noise exposure when examined using ICI with ABR, CAP and single unit SGN recordings (Liu et al., 2012; Shi et al., 2013; Song et al., 2016). Interestingly, the late development in the temporal processing difficulties corresponds to the initial damage of the synaptic ribbon and its incomplete (~80%) recovery by one month (Shi et al., 2013; Song et al., 2016).

1.6 IHC-SGN Synaptic Proteins of Interest

While synaptic repair has been documented with the recovery of synapse counts and evoked responses, it has not been investigated using more direct measures against the synaptic protein itself. Western Blotting and Real-Time quantitative Polymerase Chain Reaction (RT-qPCR) are well-recognized measures for gene expression at both the protein and the messenger ribonucleic acid (mRNA) level, respectively. The protein that makes up the ribbon is called Ribeye, but it is defined between two sections: domain A and domain B (Schmitz, Königstorfer, & Südhof, 2000; Uthaiah & Hudspeth, 2010). Domain A is a unique sequence that is believed to provide the structural support for the ribbon itself. However, domain B shares a portion of the same sequence as another protein known as C terminal binding protein 2 (Ctbp2), a known transcriptional repressor found in various cell tissues. Therefore, domain B is believed to have some enzymatic properties that involve priming the vesicles for release. Although domain B has the same sequence as Ctbp2, the latter also has an additional 20 amino acids at the N terminal. Therefore, when using detection methods based on sequencing of Ctbp2 you potentially detect the pre-synaptic Ribeye (B domain) and the Ctbp2 protein in the nucleus. There are several other proteins that are shared by the conventional synapse, but they may play different roles for the ribbon synapse.

One of these proteins is bassoon (Buran et al., 2010; Khimich et al., 2005; Uthaiah & Hudspeth, 2010). This large protein is known to anchor the ribbon complex to the active site of the pre-synaptic zone of the cell and was first used to determine the importance of the ribbon complex. Studies have used knockouts of the bassoon gene to witness higher-than-normal freely-floating ribbon complexes within the cytoplasm of the cell. This resulted in reduced amplitudes of response from the inner hair cells, suggesting that without ribbon complexes located at the pre-synaptic active zone, auditory temporal encoding would be impacted.

Another associated protein with the ribbon complex is Rab3 interacting molecule 2 (Rim2), which is also known as regulating synaptic membrane exocytosis 2 (Gebhart et al., 2010; Jung et al., 2015; Uthaiah & Hudspeth, 2010). This protein is known to cluster $Ca_v1.3$ Ca^{2+} channels around the pre-synaptic ribbon active zones. These Ca^{2+} channels are required for the process of exocytosis of the neurotransmitters. When knocked out, the lack of Rim2 causes a decrease in exocytosis for IHCs (Jung et al., 2015). Interestingly, there is previous research that suggests Rim2 is only present within immature IHCs of mice (Gebhart et al., 2010), while more recent findings suggest that Rim2 is present in the mature IHCs of mice (Jung et al., 2015). Another group has studied mice with IHCs on the verge of maturity and have found Rim2 to be present (Uthaiah & Hudspeth, 2010). Regardless, the importance of Rim2 is apparent and there is evidence to suggest that it continues to support the ribbon synapse even in maturity.

The last protein that will be investigated is Growth associated protein 43 (GAP43). This protein is involved with plastic changes and the development of neurons (Dodson & Mohuiddin, 2000). One previous study has found that when hair cells were

selectively destroyed by ototoxicity in guinea pigs, the SGNs had varying survival times after the damage on the scale of months (Dodson & Mohuiddin, 2000). However, the surviving SGNs showed an increase in size and an increase in expression of the GAP43 protein at three and six weeks post-damage (Dodson & Mohuiddin, 2000). This thesis will only look at GAP43 expression after noise damage; however, it would be interesting to research how GAP43 is regulated over time after the said noise damage. To understand the regulation of all of the previously mentioned proteins in the cochlea, varying time points will be employed to measure them along with their mRNA relative amounts to monitor changes in expression after HHL noise damage. Therefore, potential changes of the protein expression will be observed at both the translation and the transcription level using Western Blotting and RT-qPCR respectively in the attempt to provide further insight into the synaptic damage and repair.

1.7 Ribbon Repair Study

As previously mentioned, research shows that the damaged ribbon can be partially repaired after noise exposure in guinea pigs (Liu et al., 2012; Shi et al., 2013). These observations are based upon the immunostaining of ribbons using antibodies against CtBP2 (Liu et al., 2012; Shi et al., 2013). However, it is not clear if the loss of the CtBP2 signal is due to the loss of whole ribbons. Therefore, the repair could require either the synthesis of completely new proteins or ribbons could be assembled by using the broken-down molecules from the damaged ribbons. In the proposed study, as a part of a larger project in exploring the mechanisms of ribbon damage and repair, I am going to verify whether the repair of the ribbons requires the synthesis of new Ribeye protein.

The ribbon synapses in the guinea pig animal model have been shown to require about a month to recover original ribbon counts (Shi et al., 2013). Such a long recovery period suggests that more protein would have to be synthesized. Therefore, it is expected that the amount of ribbon and associated proteins will decrease in concentration after noise damage. At the same time, mRNA of the ribbon and associated proteins will be increasing in concentration to show that significant amounts are being produced to synthesize new ribbon and associated proteins. In the end the ribbon synapse protein concentration will increase to similar levels found in control samples.

Overall, the impact of NIHHL is being further examined by focusing on proteins and mRNA of the ribbon synapse in hair cells. However, no significant changes of interest were found. Trends in this research suggest that by one week post-noise exposure, some ribbon mRNA was up-regulated. This could indicate a possible repair process of the ribbon synapse, providing further evidence of repair with NIHHL. By understanding and providing further evidence for the repair process we can strive to figure out why these repaired ribbons are not functionally the same with regards to auditory temporal dysfunction. Synaptic counts were found by others in the lab to be decreased more so in the high frequency region, and AM signals with more modulation depth resulted in lower CAP responses even after one month post-noise exposure. This temporal dysfunction with exposure to noise trauma is believed to cause difficulties with peoples' hearing ability in background noise that is not detectable by traditional audiological clinical standards.

Chapter 2 Materials and Methods

2.1 Subjects and Procedure Outline

Male adult albino guinea pigs were used in this project. The major procedures were sequentially done as: (1) surgical implantation of electrodes for the recording of the CAP from the round window membrane and the ABR from the scalp, (2) baseline recording of ABR and CAP, three days after the surgery, (3) noise exposure, (4) endpoint functional evaluations at one day post-noise (DPN), one week post-noise (WPN) and one month post-noise (MPN) in the noise group and at the corresponding time of 1MPN for the control group, (5) molecular analysis in groups after the final functional tests.

Initially, the noise induced changes in cochlear responses were designed to be observed in a self-controlled manner using an implanted electrode. A total of 32 male adult albino guinea pigs were planned to be used with eight per group, and each providing one cochlea to protein analysis (Western Blotting) and the other cochlea for RNA analysis (RT-qPCR). Additional animals were included later due for several reasons: (1) to replace cochlea that could not be used (ex. premature expiration, discovery of infection upon cochlea harvesting (seven in total added for original functional analysis and used for subsequent molecular analysis)), (2) to quantify the noise induced change in the ribbon synapse count and to evaluate the noise-induced changes of cochlear responses in a between-group design (n=14, 7 each in the control and the noise group, observed at 1MPN).

Eventually, a total of 53 guinea pigs were used in this project. They were recruited at the age of 1-2 months (300-350 g in body weight) from Charles River Co,

Canada. All the procedures were approved by the university committee of laboratory animals of Dalhousie University.

2.2 Electrode Implantation

The guinea pigs underwent electrode implantation surgery by others in Dr. Wang's lab, one week after receiving them. The animal was anesthetized with ketamine and Xylacine (40-60 mg/kg +10 mg/kg respectively intraperitoneal (IP)). Using a thermostatic heating pad, the body temperature was kept at 38.5^{o}C during the surgery. After anesthesia induction, 0.5 ml of 1% lidocaine was injected subcutaneously in the post-auricular area. A 2 cm skin incision was made and the connective tissue and muscles were retracted to provide exposure of the mastoid bulla. A hole of 2-3 mm in diameter was punctured through the mastoid to expose the round window niche of the cochlea. CAP was recorded via a silver-wire electrode that was placed on the round window membrane. The electrode was made from Teflon-coated silver wire (0.003 inch in diameter, Cat#75810, A-M System Inc.). The insulation was cut off by 2 mm at the tip and the naked wire was coiled to make a ring. The other end of the silver wire was soldered to a pin head. The wire was fixed with dental cement to the mastoid with the help of a small screw that was inserted into the temporal bone. A piece of head skin of 1x2 cm^2 in size was cut off to expose the skull surface at the vertex. The soft tissue was cleaned with a scalpel and 10% H_2O_2 solution. Three small holes were drilled on the scalp to implant the recording, reference and grounding electrodes for both ABR and CAP as illustrated in Figure 1. The skull-insert electrodes were made of Tungsten wire of 0.3 mm diameter and soldered to a pin head. All the pinheads, including the two from the round window of both ears for CAP, were fixed to the skull with dental cement.

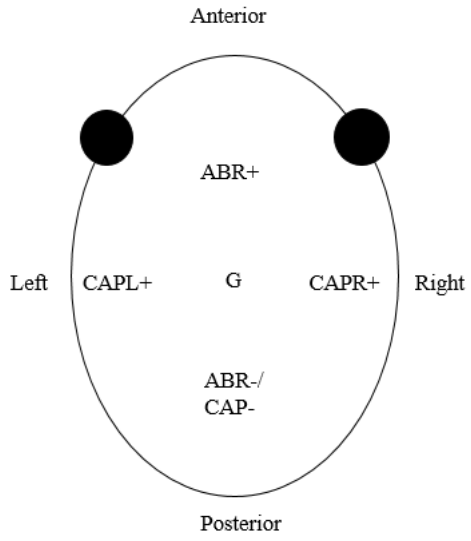

Figure 1. Electrode placement with horizontal view of the head. Measurements include active electrodes for compound action potential for both left and right round window (CAPL and CAPR, respectively), electrodes for auditory brainstem response (ABR) and an electrode for grounding (G).

2.3 Electrophysiology Tests

The animals were anesthetized with ketamine mixed with xylazine (40mg/kg and 4 mg/kg, IP) and the body temperature was maintained at 38 ºC with a thermostatic heating pad by others in Dr. Wang's lab. Hardware and software from Tucker-Davis Technologies (TDT System III; Alachua, FL, USA) were used for stimuli generation and bio-signals acquisition. The acoustic stimuli used were as follows: (1) clicks for CAP (0.1-ms duration, presented at the rate of 21.1/s), (2) tone bursts for ABR and CAP (10-ms duration with $\cos^2$ gating and 0.5-ms rise/fall time, at rate of 21.1/s), and (3) 20 kHz AM tones for CAP (500-ms duration with rise/fall time 5 ms, at rate of 1.5/s). The stimuli were played out through a broadband speaker (MF1; TDT) and was delivered to

the tested ear via a 10-cm tubing. For ABR tests and CAP input/output (I/O) functions, the sound level was decreased in 5-dB steps from 90 dB SPL until the response disappeared. For AM CAPs, the sound was presented at 80 dB SPL with modulation frequencies at 93 and 996 Hz respectively. The evoked responses were led to the PA16 preamplifier of the TDT system by using cables with female pin heads. The biological signals were amplified by 20X in the preamplifier, digitized and filtered between 100 and 3,000 Hz for click and tone burst ABRs, or between 10 and 3,000 Hz for AM CAPs. The responses were averaged over 1000 responses for ABRs and 100 for CAPs. The ABR thresholds were tested at 1, 2, 4, 8, 16 and 32 kHz, and were defined as the lowest level where a repeatable wave III response was detected. The AM CAP was measured by detecting the peak of modulation frequency in the spectrum analysis of the averaged 500 ms sweep after the first and the last 50 ms of responses were cutoff.

2.4 Noise Exposure

The animals were placed in a metal-wire cage, awake and unrestrained, during the noise exposure. Gaussian noise was generated and was high-pass filtered with cutoff at 4 kHz by RP2 signal processor from Tucker-Davis Technologies (TDT System III; Alachua, FL, USA). The output of the signal processor was amplified by an audio-amplifier (Crown XTi6002, USA) and delivered to a four-speaker array (Pyramid TW-67 tweeters, Amazon.com) suspended 40 cm above the animals. The exposure was given at 105 dB sound pressure level (SPL) for two hours. The acoustic spectrum of the noise was distributed mainly between 4 and 22 kHz (Figure 2). The noise level was monitored using a 1/4-inch microphone linked to the RP2 module of the TDT system through which the sound level was calculated by an RPvdx circuit.

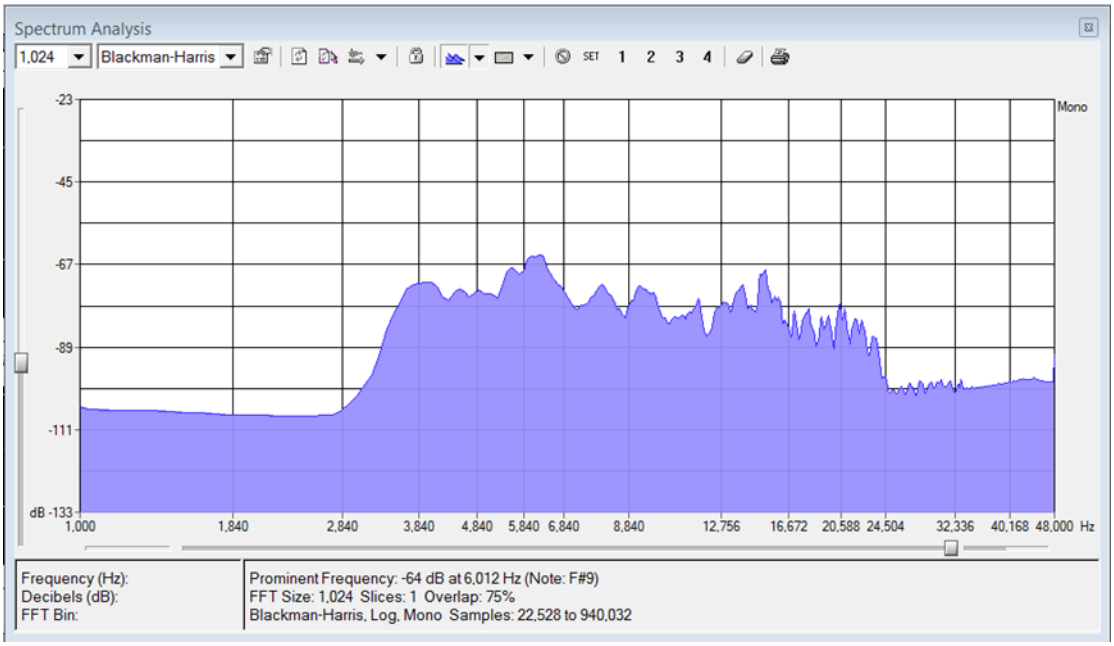

Figure 2. The spectrum of the high-pass filtered noise used in this project.

2.5 Morphology for Ribbon Synapse Counts

Following the endpoint physiological tests, the animals were sacrificed with an overdose of pentobarbital (100 mg/kg, i.p.) and these cochleae were harvested by others in Dr. Wang's lab. The cochleae were quickly harvested and perfused rapidly with 4% paraformaldehyde in phosphate-buffered saline (PBS), and immersed in paraformaldehyde for one hour fixation at 4 ˚C. Then each cochlea was transferred into PBS, and the bony shell of the cochlea was removed with fine forceps. After removing the tectorial membrane, it was permeabilized with 1% Triton X-100 in PBS for 60 mins, and then incubated in 5% goat serum in PBS for another 60 mins. The cochlear basilar membrane was incubated with the mixture of mouse anti-CtBP2 antibody (IgG1; BD Biosciences, cat. # 612044, 1:200) and mouse anti-PSD95 antibody (IgG2a; Millipore, cat. # MAB1596, 1:600). After stored overnight at 4 ˚C, the PBS-washed cochleae were treated with corresponding secondary antibodies (goat anti rabbit IgG, goat anti mouse

IgG1 and IgG2a, 1:800, Invitrogen A11034, A21124 and A21131 respectively) for two hours at room temperature. After immunostaining, the cochleae were post-fixed with paraformaldehyde again for 60 mins. The basilar membranes were dissected in four pieces and mounted on the microscope slides. The basilar membrane for transfection efficiency evaluation was further counterstained with DAPI (Fluoroshield with DAPI; sigma-aldrich, cat# F6057) and coverslipped. Confocal images at the specific frequency position (1, 2, 4, 5.6, 8, 11.3, 16, 22.6 and 32 kHz) were acquired using a confocal laser-scanning microscope (LSM 710 META; Zeiss, Shanghai, China) with the 63× water-immersion objective. Image stacks were then exported to image-processing software, ImageJ (NIH), and eight successive IHCs at each frequency position of the cochleae were selected to count their puncta of CtBP2 (in red) and PSD95 (in green).

2.6 Molecular Analysis

The gene expression data were obtained successfully from a total of 39 animals, from which 39 cochleae were used for protein analysis and 37 for RNA analysis. Table 1 summarized the number of cochleae used across the four different conditions including a no noise control group, and three time points after noise exposure, one day post-noise (DPN), one week post-noise (WPN) and one month post-noise (MPN).

Table 1. Number of cochleae per condition harvested and usable after validation experiments.

Condition	Number of cochlea	
	Protein Analysis (Western Blotting)	RNA Analysis (RT-qPCR)
Total	39	37
Control (no noise)	8	8
1 Day post-noise (DPN)	10	10
1 Week post-noise (WPN)	10	8
1 Month post-noise (MPN)	11	11

2.6.1 Reagents

UltraPure™ Dnase/RNase free distilled water (10977015), glycine (56-40-6), methanol (67-56-1), ethanol (64-17-5) and protease inhibitor (A32957) was obtained from ThermoFisher Scientific (Ottawa, ON). Aurum™ total RNA Fatty and Fibrous tissue module (7326870), Clarity™ Western ECL Substrate (1705060), Experion RNA StdSens Analysis kit for 10 chips (7007103), Precision Plus Protein™ All Blue Prestained Protein Standards (1610373), Protein assay dye reagent concentrate (5000006), Protein standard 1 (5000005), PureZOL™ RNA isolation reagent (7326890), SsoFast™ EvaGreen® Supermix (1725203), 2-mercaptoethanol (1610710), 2xLaemmli Sample buffer (1610737) and 4-15% Mini-PROTEAN™ TGX Stain-Free™ protein gels, 15 well (4568086) from Bio-Rad (Mississauga, ON) were ordered. Tris buffer (77-86-1) was obtained from Roche Diagnostics (Mississauga, ON). RIPA buffer (9806s) was obtained from Cell Signaling Technology (Danvers, MA). Sodium chloride (7647-14-5) was obtained from EM

Science. Tween 20 (9005-64-5) was obtained from Sigma (Oakville, ON). Pentobarbital from Ceva was used. Additionally, powered skim milk was purchased locally.

2.6.2 Western Blotting

Western Blotting was used to determine the protein concentration during the various time points (Taylor, Berkelman, Yadav, & Hammond, 2013; Taylor & Posch, 2014). Overall, Western blotting involves creating a three-dimensional picture. Firstly, each sample is separated by loading them in a different lane in a gel. Secondly, each protein is separated based on the size (weight) of the different proteins present in a sample by way of applying an electric field across the gel. The porous gel allows protein movement when an electric field is applied, with larger proteins moving more slowly than smaller proteins. Upon transferring the separated proteins from a gel to a membrane, antibodies can be applied to detect specific proteins. The third dimension is the intensity of the detected proteins by way of the antibodies. The darker the signal, the more concentrated that specific protein is within that sample. Therefore, this technique can be used to determine the relative amounts of specific proteins by looking at the fold difference which compares an experimental sample to a control sample.

2.6.2.1 Protein Extraction

BeadBug™ microtube homogenizer from Benchmark Scientific with BeadBug™ prefilled tubes, 2.0 mL capacity with 2.8 mm stainless steel beads, acid washed from Millipore Sigma (Z763829), were used to homogenize the cochleae. At the designated time point, animals were sacrificed with an overdose intraperitoneal (IP) injection of ketamine/pentobarbital and then if necessary, a cardiac injection. The first cochlea harvested was used for RNA analysis and the second for protein analysis. The second

cochlea was placed in BeadBug™ prefilled tubes with 100 µL of RIPA buffer. The tube was shaken at max speed for 30 seconds with a microtube homogenizer. The resultant mixture was pipetted out as much as possible and then spun down in a centrifuge. The supernatant was then removed and placed in separate tube and stored at -80 ˚C.

2.6.2.2 Protein Assay

The protein assay was completed as described in the protocol for the Bio-Rad Protein Assay when using Bio-Rad's protein assay dye reagent concentrate (5000006). Specifically, the microassay procedure for microliter plates was followed. This spectrophotometric technique was used to determine the total protein concentration of extracted samples, using Bio-Rad's Protein standard 1 (5000005). All samples, including the standard, were tested in triplicates. Basically, using the known concentration of the standard, a calibration curve was generated by measuring their specific absorbance when a specified wavelength of light was used. Samples of interest were then diluted appropriately and measured against the calibration curve.

2.6.2.3 SDS-PAGE

Sodium dodecyl sulfate-polyacryamide gel electrophoresis (SDS-PAGE) was utilized to separate proteins by size. Specifically, Mini-PROTEAN™ TGX Stain-Free™ protein gels, 15 well (4568086) from Bio-Rad were used. Due to the wide range of sizes for the proteins of interest, a pre-cast gradient gel of 4-15% was used. Note a pooled sample was made by taking 2 µl of each protein sample to be tested to be used for total lane normalization. SDS PAGE running buffer was used during the protein separation (120 mM Tris, 0.7 M Glycine, 17 mM SDS).

Protein samples were prepared with Laemmli sample buffer and 2-mercaptoethanol as described in the protocol provided with these reagents. For protein size determination, 10 µl of the Precision Plus Protein™ All Blue Prestained Protein Standards (1610373) was pipetted in a lane. The gel was run for 30 minutes at 200 V. Right after running the gel, it was taken to have the stain (for total lane normalization) activated in UV light using a ChemiDoc™ Imaging System (17001401) from Bio-Rad. This step also allowed for checking to see if proper protein separation was achieved before transferring the proteins to a membrane.

2.6.2.4 Protein Transfer

A Tris (tris(hydroxymethyl)aminomethane)/glycine/methanol transfer buffer (25 mM Tris, 0.2 M glycine, 20% methanol) was used to transfer proteins with a polyvinylidene fluoride (PVDF) 0.2 µm membrane from EMD Millipore (Etobicoke, ON). Protein transfer was done for 2 hours at 100 V with ice surrounding the apparatus. The image of the membrane, for total lane normalization, was taken right after with a ChemiDoc™ Imaging System.

2.6.2.5 Protein Detection with Antibodies

The antibodies used were anti-Rim2 (100842) from Santa Cruz Biotechnology (Mississauga, ON), anti-GAP43 (G9264) from Sigma (Oakville, ON), anti-Bassoon (141021) and anti-ribeye A domain (192103) from Synaptic Systems (Germany), and anti-Ctbp2 (612044) from BD Biosciences (Mississauga, ON). The secondary antibody was anti-Mouse IgG (Fab specific)–Peroxidase antibody produced in goat (A2304) from Sigma (Oakville, ON).

Membranes were blocked in 5% powered skim milk that was dissolved in Tris buffered saline with Tween-20 (TBS-T; 2.5 mM Tris, pH of 7.5, 15 mM NaCl, 0.01% Tween-20) on a shaker for one hour. The blocking solution was changed three times. The primary antibody was diluted at 1:2000 in 2% milk in TBS-T blocking solution. The membrane was shaken for one hour at room temperature. It was then shaken overnight at 4 °C in a walk-in fridge. The next day it was shaken at room temperature for one hour (still in the primary antibody). It was taken out of the antibody solution and rinsed twice in TBS-T. It was then shaken in TBS-T for 15 minutes, then shaken for five minutes with fresh TBS-T and this was repeated three times. The secondary antibody, anti-mouse, was diluted (1:5000) in 2% milk in TBS-T blocking solution. Membranes were then shaken at room temperature for one hour. Next, the membranes were washed as described previously for the primary antibody.

Bio-Rad's Clarity™ Western ECL Substrate (1705060) was used to visualize the antibodies. First, a sheet protector was cut on two sides so that it can be opened like a book and the membrane was placed on the open sheet protector. Then, ECL substrate solution was pipetted on the membrane and the sheet protector was closed on top to ensure an even coating of ECL. This was left to sit for 5 minutes. Afterwards, membranes were visualized with a chemiluminescent reading and then a colourmetric one for the protein ladder using a ChemiDoc™ Imaging System.

2.6.2.6 Protein Lane Loading Standardization

A serial two-fold dilution was used to test loading total protein amounts from 2.5-80 µg. This procedure is used to determine the amount of total protein that falls within a detectable linear range.

2.6.3 RT-qPCR

The quantification of nucleic acids has been made efficiently possible thanks to the development of qPCR (quantitative polymerase chain reaction) (Bustin et al., 2009; Taylor, Wakem, Dijkman, Alsarraj, & Nguyen, 2010). Whether one is working with DNA or RNA (reverse transcription, RT-qPCR), this relative quantification technique utilizes an intercalating dye that activates when newly produced complimentary DNA (cDNA) is made. Only specific cDNA is produced by the presence of selective primers that are designed specifically for a pre-determined sequence. By monitoring the dye activation by a doubling of cDNA every pre-determined thermal cycle, one can determine this relative amount of a specific sequence when compared between controls.

2.6.3.1 RNA Extraction/purification

The first cochlea was placed in BeadBug™ prefilled tubes with 1mL of PureZol lysis buffer. The tube was shaken at max speed for 30 seconds with a microtube homogenizer. The tube was then left to sit at room temperature for five minutes. Then the resultant mixture was pipetted out as much as possible and then spun down in a centrifuge under -4˚C. The supernatant was then removed and placed in a separate tube and stored at -80 ˚C.

2.6.3.2 RNA Quantity Assessment

RNA quantity was assessed using spectrophotometric techniques on a BioTek Epoch™ UV-Vis Spectrophotometer. By taking readings at several wavelengths of samples, total RNA quantity can be determined (Taylor, 2016). This value was used to dilute all samples to the same concentration before converting the RNA to cDNA.

2.6.3.3 RNA Quality Assessment

RNA quality was assessed using Bio-Rad's Experion™. This system uses a gel electrophoresis technique to detect two bands, 28S and 18S, present within high quality RNA (Taylor, Wakem, Dijkman, Alsarraj, & Nguyen, 2010). The ratio of intensity of these bands are used to give an RQI value which gives a value of RNA quality. Any samples with a RQI value less than seven was excluded for poor quality.

2.6.3.4 RNA Reverse Transcription to cDNA

Bio-Rad's iScript™ cDNA Synthesis kit (1708891) was used to convert RNA to cDNA with an Eppendorf Mastercycler. The procedure for this kit was followed as provided by the company. Note, 1 µg of the total RNA was used from each sample to convert to cDNA.

2.6.3.5 Primer Design

For both potential reference genes and genes of interest, messenger ribonucleic acid (mRNA) sequences were obtained from the online National Center for Biotechnology Information (NCBI) database (US National Library of Medicine, 2017a). It should be noted that these sequences were sometimes partial and/or theoretical. However, for the purpose of primer design, entire sequences of particular genes is not required. The obtained mRNA sequences were then applied to an online software called Primer3 to design primers (Koressaar & Remm, 2007; Untergasser, Cutcutache, Koressaar, Ye, Faircloth, Remm & Rozen, 2012). Note, no setting adjustments were done to Primer3 (v. 0.4.0; http://bioinfo.ut.ee/primer3-0.4.0/).

For the purpose of reference genes, the four most stable determined genes (Table 2) were selected from a previous study that looked at expression before and after noise

exposure in the inner ear (Melgar–Rojas, Alvarado, Fuentes–Santamaría, Gabaldón–Ull, & Juiz, 2015). It should be noted that this study used rats, however no study on reference genes for noise exposure in guinea pigs could be located.

Next, designed primers were cross-checked for specificity using online Primer-BLAST software available through NCBI (US National Library of Medicine, 2017b). This is to ensure that a primer only amplifies a specified genetic target. Table 2 shows the chosen primers for each gene of interest and potential reference gene tested. Primers were then ordered/manufactured from Invitrogen (A15612).

After ordering, primer pairs were reconstituted separately in 40 μM stocks in TE (TRIS-EDTA) buffer. Then both forward and reverse primer pairs were combined at 4 μM.

Table 2. List of genes and their primer sequences for RT-qPCR experiments.

	Gene	NCBI Gene Reference Number	Primer Sequence (5'-3')	Amplicon Length (bp)
Potential Reference genes	beta-2-microglobulin (B2m)	XM_005006080.2	F: GCATCTGGACACAGGGAAGT R: GGTACAGCAACTGCCTCACA	195
	Hypoxanthine phosphoribosyltransferase 1 (Hprt1)	XM_003462671.3	F: TGATCAGTCAACAGGGGACA R: AAGCTTGCGACTTTGACCAT	168
	Ribosomal protein, large, P0 (Rplp0)	XM_003478381.3	F: GCGACCTGGAAATCCAACTA R: GGCAACAGTTTCTCCAGAGC	221
	TATA box binding protein (Tbp)	XM_013148964.1	F: GCCCGAAACGCTGAATATAA R: CCAAGAATTTGGCTGGAAAA	196
Genes of Interest	Bassoon (Bsn)	XM_003476451.3	F: CCCCTGTGTCTTTCACCACT R: GGCTGGACAAGGAGCTACAG	218
	C-terminal binding protein 2 (Ctpb2)	XM_013143420.1	F: CCAGTGCCCAACTATGGAGT R: GGCATCTGGCAGTTCTCTTC	186

	Gene	NCBI Gene Reference Number	Primer Sequence (5'-3')	Amplicon Length (bp)
Genes of interest	Growth associated protein 43 (Gap43)	XM_013151711.1	F: GTGTGTGCAATGTTCCGTTC R: AGCCATAGAGCCGCAAGTTA	204
	regulating synaptic membrane exocytosis 2 (Rim2)	XM_013143998.1	F: GATCTCCCGTGTGTGTTCCT R: CAGCAGTGGTCACCAGCTTA	197

2.6.3.6 Primer Annealing Temperature

Primers were designed to optimally perform at 60°C. However, to ensure that this temperature is appropriate, primers were tested with a pooled cDNA sample at various temperatures ranging from 53 to 65 °C in duplicates using a gradient procedure on a Bio-Rad CFX96^{TM} Real-time PCR system. This annealing temperature refers to the optimal temperature the newly made DNA sequences recombine after heat exposure and before reading the qPCR dye that has been chelated in this process (Taylor, 2015). An optimal temperature range was found by visually looking for the lower/lowest cycle threshold (C_q). From this optimal range, the temperature that was tested that fell into this range for each primer pair was chosen as the experimental annealing temperature.

2.6.3.7 Primer Melt Curve

Melt curves were generated after amplification of the cDNA product was complete. This allows for the chelated dye to deactivate as the DNA product is degraded. This response is recorded and if more than one peak is detected, then more than one product is being produced and the primers are not specific enough (Taylor et al., 2010). The melt curve procedure was followed as suggested by the company for Bio-Rad's CFX96^{TM} Real-time PCR system by ramping temperature from 65-95°C in 0.5 °C increments.

2.6.3.8 Primer Standard Curve

Standard curves were generated using pooled samples of cDNA. They were done in triplicate, ranging from 1/10 to 1/21870 in a serial dilution of the original cDNA sample. To be acceptable primers, a standard curve had to be generated that had an efficiency ranging from 90-110% and an r^2 greater than 0.98 (Bustin et al., 2009; Taylor et al., 2010). Primer pairs that did not meet this requirement were excluded from analysis.

2.6.3.9 Reference Gene Stability

Reference genes are utilized to normalize the qPCR data, but to use them they must have a certain stability (Bustin et al., 2009; Taylor et al., 2010). To ensure their stability, several programs were used including Bio-Rad's CFX Manger, NormFinder and BestKeeper (Andersen, Jensen, & Ørntoft, 2004; Pfaffl, Tichopad, Prgomet, & Neuvians, 2004).

2.6.3.10 RT-qPCR Cycle Thresholds

For the final experiment, each biological sample had three technical replicates. If the standard deviation of the technical replicates exceeded 0.2, then the outlier technical replicate was removed if doing so improved (lowers) the standard deviation. In the case that two of the three technical replicates do not amplify any product, that biological sample was removed from analysis. This occurred for one control and one day sample from the Ctbp2 analysis. For the final experiment, pooled samples of RNA were tested in triplicates for each primer for the presence of genomic DNA contamination. These were called no-reverse transcriptase controls (NRT). Additionally, water samples were tested with qPCR reagents to test for contamination and these were called no-template controls (NTC).

2.7 Data Analysis

Statistics were done using SPSS software (Version # 23). Western Blot and RT-qPCR data was assessed by doing a Kruskal-Wallis One-Way Analysis of Variance (ANOVA) and Mann-Whitney test for post-hoc analysis (Goni, García, & Foissac, 2009; Yuan, Reed, Chen, & Stewart, 2006). Functional and morphological evaluations were analyzed by ANOVA or t-test whichever was appropriate. A statistical significance alpha of 0.05 was used for Kruskal-Wallis testing, with an alpha of 0.016 (0.05/3) for post-hoc using the Bonferroni procedure (Haynes & Johnson, 2009, p. 177-178). These non-parametric statistical tests were chosen since unequal group sizes were obtained by the end of the experiment due to uncontrollable factors (Table 1).

Chapter 3 Results

3.1 Reduced Cochlear Output After Noise Exposure

The hearing thresholds of the animals were measured with tone-burst evoked ABR across a frequency range from 1 to 32 kHz in octave steps (Figure 3). The noise exposure produced significant threshold elevations only at one day post-noise exposure (DPN). The frequency-threshold curves of the control (Ctrl), one week post-noise exposure (WPN) and one month post-noise exposure (MPN) were overlapped. A two-way ANOVA was performed against the factor of grouping (reflecting the role of noise) and frequency. The post-hoc pairwise comparisons (Bonferroni method) showed significant differences between the thresholds at 1DPN and the controls at frequencies above and equal to 4 kHz ($p<0.001$). All other pairs were not significantly different.

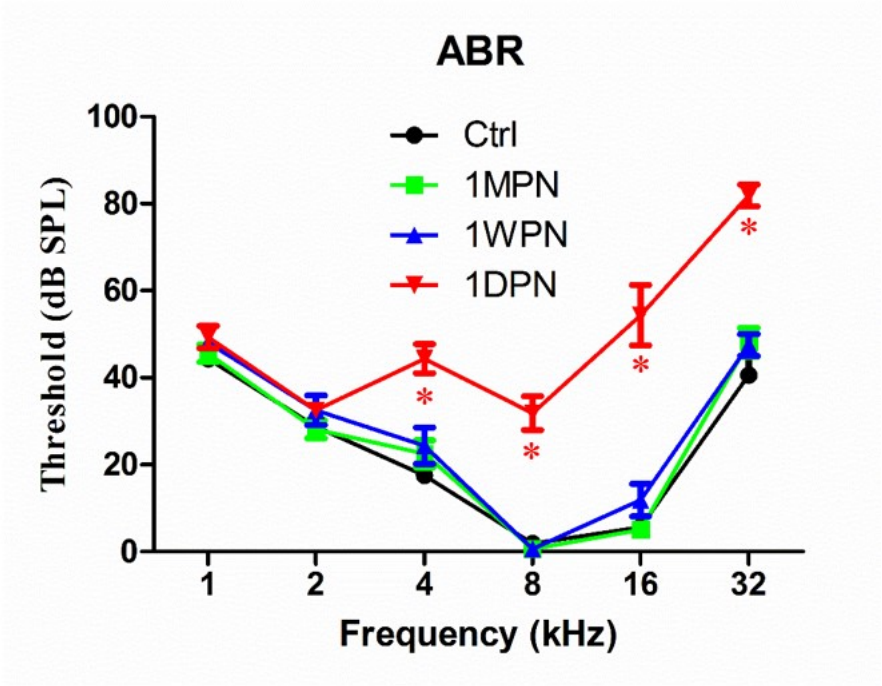

Figure 3. ABR threshold changes and recovery after the noise exposure. Therefore, noise exposure only caused a temporary threshold shift. N=7 in each group. *: $p<0.001$.

Cochlear responses to clicks, tone bursts and AM signals were evaluated via round window electrodes at 1MPN just before the animals were sacrificed for morphologic observations. The input/output function of CAP to clicks and 20 kHz tone bursts are summarized in the upper panel of Figure 4. The CAP amplitudes obtained at 1MPN were significantly lower than the corresponding values of the control group. The averaged maximal click CAP was 875.49 ± 45.31 microvolts (μV) for the control group, and 402.37 ± 30.12 μV for the noise group. The average maximal CAPs evoked by 20 kHz tone bursts were 176.54 ± 35.56 and 105.44 ± 28.95 for the control and the noise groups respectively. As compared with the control group, the click CAP was 54% lower ($t=8.684$, $p<0.001$), and the tone burst CAP by 40% ($t=3.798$, $p=0.003$). The AM CAP was tested with a 20 kHz carrier frequency at 80 dB SPL. The amplitude-modulation depth curves were overlapped between the control and the noise groups with a modulation frequency of 93 Hz. However, the response was reduced in the noise group when the modulation frequency was 996 Hz. The amplitude tested at 100% modulation depth was 111.30± 10.81 μV and 44.98 ± 5.27 μV for the control and the noise groups respectively, with the noise group having dropped by 60% ($t=5.515$, $p<0.001$).

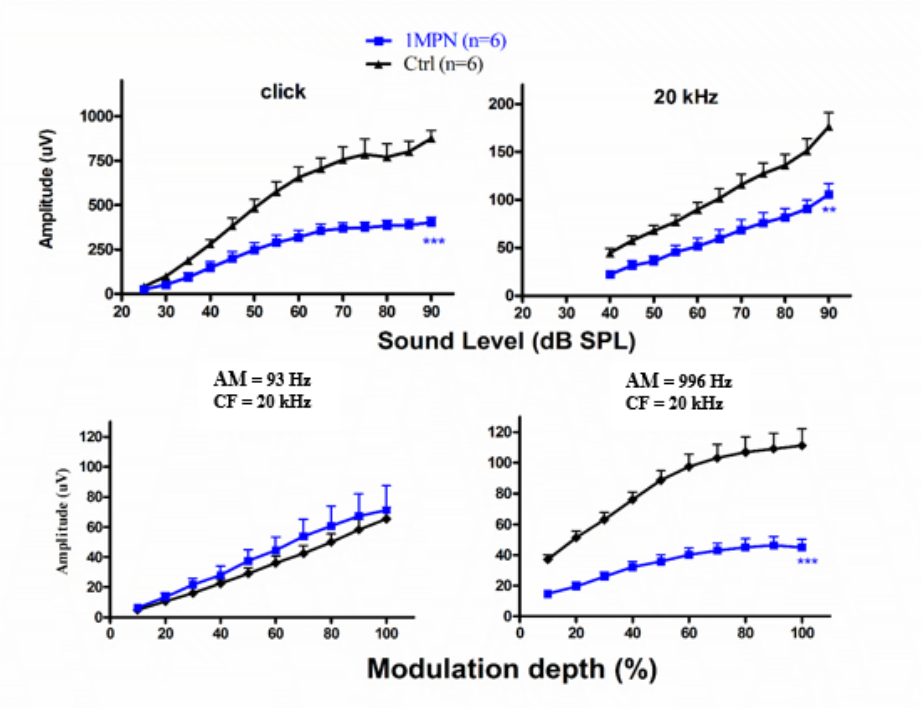

Figure 4. Between-group comparison of CAP recorded from the round-window at 1MPN. Upper panel: CAP evoked by click (left) and 20 kHz tone burst. Lower panel: CAP evoked by 20 kHz carrier frequency (CF) (at 80 dB SPL) modulated by 93 Hz (left) and 996 Hz (right) respectively. The between-group comparison was statistically tested with two sample t-tests at 90 dB SPL for click and tone burst and at 100% modulation depth for 20 kHz AM. Reduced cochlear output was found, especially at higher intensities and amplitude modulation depths. **: $p<0.01$, ***: $p<0.001$. N=6 in each group.

3.2 Noise Damage on Ribbon Synapses

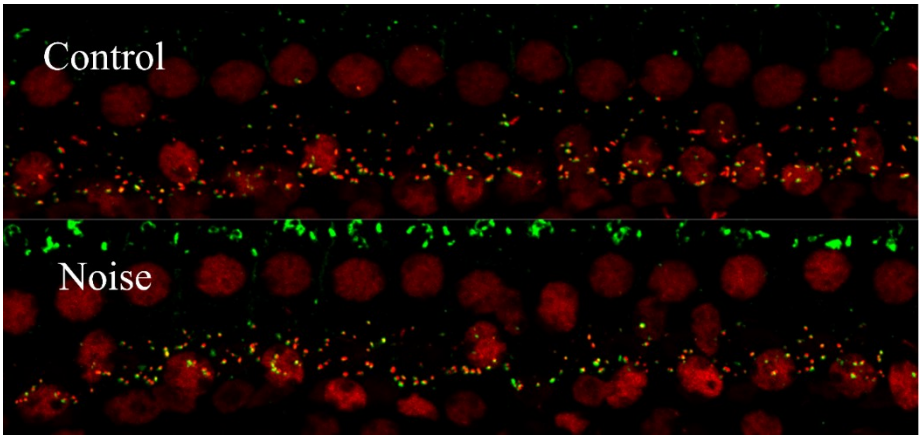

Figure 5. The selective images of immunostaining against the presynaptic ribbons (labeled by antibody to CtBP2, red) and the post-synaptic terminals (labeled by antibody to PSD95, green).

Figure 5 and 6 compared the synaptic counts between groups obtained at 1MPN. Synaptic counts were expressed with the density of both pre-(CtBP2) and post-synaptic (PSD) puncta (#puncta/IHC) as a function of frequency location. As shown in Figure 5, both the pre- and post-synaptic puncta were paired, so both of the counts showed similar differences between groups. Significant difference was seen in the synapse count in the high frequency region above 8 kHz using two-sample t-tests. For example, the CtBP2 puncta at the frequency position of 22.6 kHz were 18.4 ± 0.3, and 15.7 ± 0.5 per IHC for the control and the noise groups. A two-sample t-test revealed a statistical difference between control and noise groups at this frequency ($p<0.001$, both for CtBP2/PSD). On average, the synapse counts were reduced by ~16.3%.

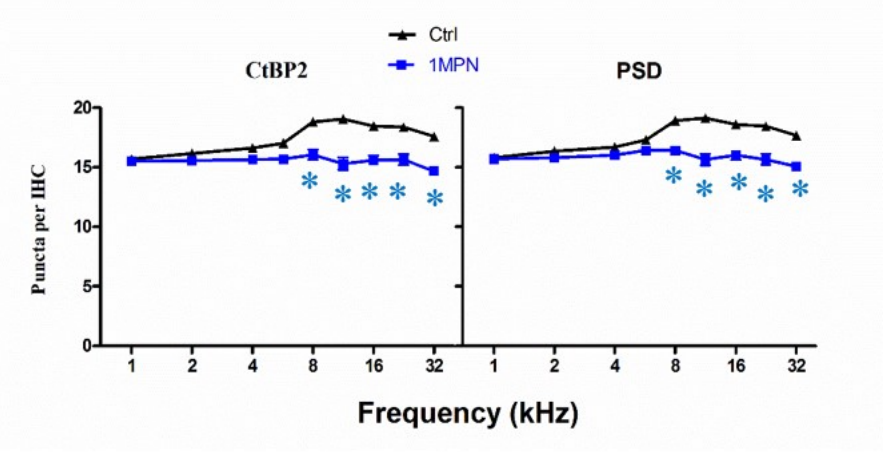

Figure 6. Comparison on synapse count cochleograms between groups. The density of synapse per IHC was expressed in the number of CtBP2 and PSD puncta per IHC as a function of frequency (location). Two sample t-tests showed significant difference (*) in CtBP2 density above and equal to 8 kHz. Therefore, significant reductions in the number of ribbon proteins (as indicated by CtBP2) and PSD were found even one month after noise exposure.

3.2 Down-Regulation of GAP43 Soon After Noise Exposure

Analyzing with and without reference genes has shown no significant differences in expression beside down-regulation for GAP43 (Table 4). Interestingly, both analyses have shown significant down-regulation at 1 DPN for this gene. This is perceived to give more credence to this difference in expression. However, only when no reference genes are used do we see a significant difference at 1 WPN for GAP43. Therefore, one should be cautious looking at 1 WPN, though the trend is present for both analyses (Figure 7). With regards to the other genes of interest, no significant difference from noise exposure was detected (Table 4).

Table 3. RT-qPCR expression results. Dashes indicate no significant change in expression. Only significant down-regulation for GAP43 was found at 1 DPN and 1WPN.

Gene of Interest	Condition	Expression Compared to Control with Reference Genes	Expression Compared to Control without Reference Genes
Bassoon	Day	-	-
	Week	-	-
	Month	-	-
Ctbp2	Day	-	-
	Week	-	-
	Month	-	-
Rim2	Day	-	-
	Week	-	-
	Month	-	-
GAP43	Day	Down-Regulated (p=0.002)	Down-Regulated (p=0.001)

	Condition	Expression Compared to Control with Reference Genes	Expression Compared to Control without Reference Genes
GAP43	Week	-	Down-Regulated (p=0.012)
	Month	-	-

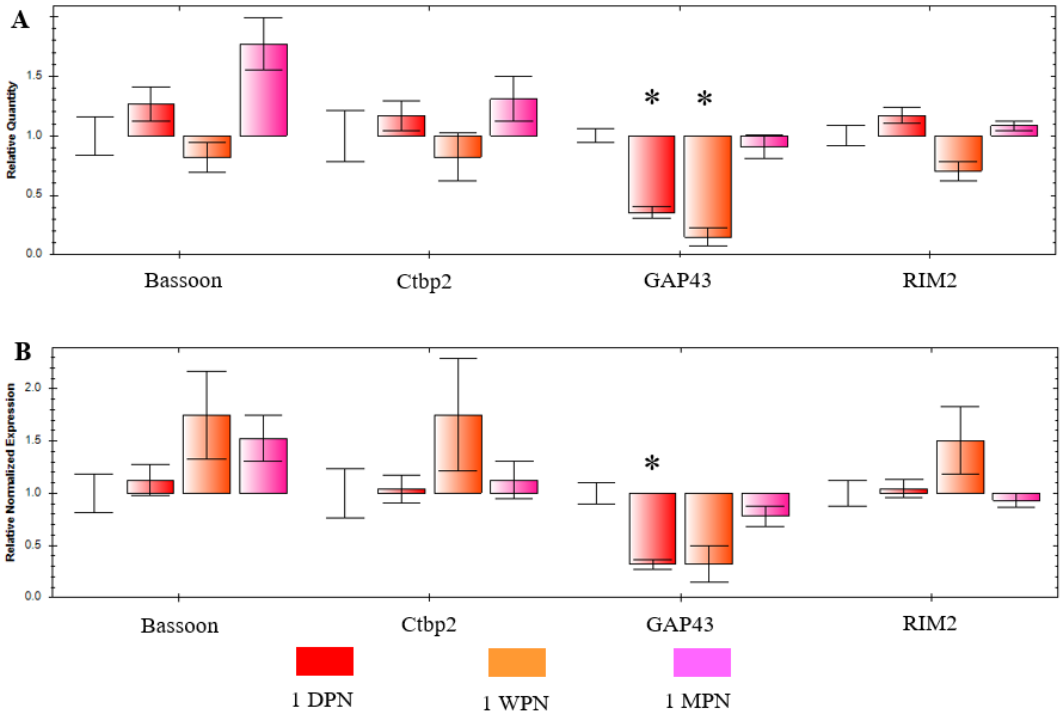

Figure 7. RT-qPCR results with (A) using no reference genes and (B) using reference genes (+/- 1 SEM). Note that error bar without a colour belongs to the control group. *: $p < 0.1$.

3.3 Inconclusive Ribbon Protein Expression

The proteins of interest tested were Bassoon, Gap43, Ctbp2 (Ribeye B domain), Rim2 and Ribeye (A domain). However, even though multiple attempts to detect Bassoon, Ribeye (A domain) and Rim2 were done, no bands were found (data not provided). Gap43 and Ctbp2 antibodies did produce bands, although the bands from the Ctbp2 antibody were not desirable. No significant differences were found for bands that were detected (Figure 8). However, due to the lack of finding a linear loading range for each protein of interest, we cannot draw conclusions from the lack of significant differences, which will be discussed later.

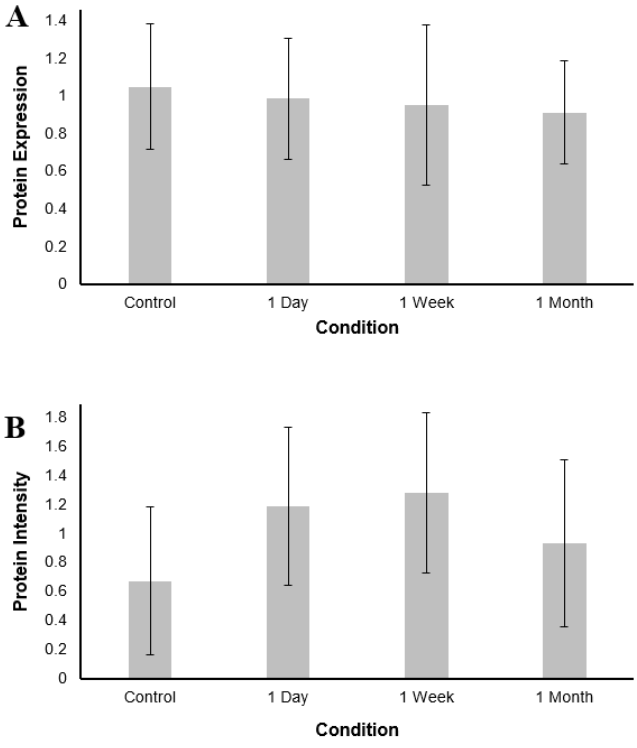

Figure 8. Normalized fold difference of protein expression grouped by condition (+/- 1 standard deviation, SD). **(A)** Ctbp2 results. **(B)** GAP43 results. No significant differences were found, however experimental setbacks prevent us of suggesting that this result is indicative of no change in protein expression (see discussion for more details).

Chapter 4 Discussion

For the purpose of this research, guinea pigs were selected as the animal to be studied for several reasons. Firstly, the people in the lab have experience working with these animals. Secondly, the ribbon synapse recovery has been found in guinea pigs, but not mice (Kujawa & Liberman, 2009; Liu et al., 2012; Shi et al., 2013; Song et al., 2016). Since the goal of this research is to study the repair mechanisms of the ribbon synapse from HHL noise trauma, it is pertinent to continue looking at the guinea pig. Additionally, previous research has noted the low concentrations of ribbon synaptic proteins (and therefore consequently mRNA) of hair cells, and the guinea pig has a larger cochlea than the rat (Albuquerque, Rossato, Oliveira, & Hyppolito, 2009; Uthaiah & Hudspeth, 2010). The larger the cochlea the more potential protein that can be harvested, thus making proteins and mRNA more detectable. Guinea pigs have been used previously for otologicial research, due to the morphological similarities to the human auditory system (Albuquerque et al., 2009).

In this project, cochlear synaptopathy was created by using a similar noise exposure to that used previously (Liu et al., 2012; Shi et al., 2013), which caused no PTS. The CAP amplitude evaluated 1MPN was significantly lower than that of the control group. The CAP amplitude reduction at 90 dB SPL was 54% for a click and 40% for a 20 kHz tone burst. A significant amplitude reduction in AM CAP was seen with a high modulation frequency close to 1 kHz but not with a low modulation frequency. The reduction at 100% modulation depth in the noise group was ~60% as compared with the control value when the 996 Hz modulation was used. The remaining synapse counts at 1MPN was comparable with the previous results and the reduction was limited to 16% in

the high frequency region (>=8 kHz), which was much smaller than the functional decrease in the CAP amplitude.

The results of this study provided new functional evidence for how the synaptic repair, after initial synaptic damage by the noise, impacts the cochlear function. In previous studies with guinea pigs, the synaptic density was reduced by more than 50% in the high-frequency region when observed at 1DPN (Shi et al., 2013). This result suggests that the noise damage is not limited to the synapses innervating low-SR auditory nerve fibers (ANFs). This is proposed since low-SR units are only a small portion of the total amount of ANFs (Liberman, 1978) and do not make significant contributions to the CAP, which is the synchronous response to the onset of sound (Bourien et al., 2014). The synaptic count shows some but not complete recovery at 1MPN. More importantly, the recovery of the cochlear response amplitude is smaller than the recovery of the synapse count. This difference suggests that the repaired synapses are functionally abnormal.

However, as mentioned by Bourien et al., low-SR units can be defined differently (2014). Bourien et al. (2014) categorizes them into low, medium and high-SR units, however Furman et al. (2013) groups the low and medium-SR units together. The latter found low-SR units contributing to the CAP response and the former did not, but they each used different definitions to categorize the ANFs. Furman et al. (2013) determined that lower-SR units (ANF categorization of low and medium-SR units according to Bourien et al., 2014) were more sensitive to noise damage. Therefore, medium-SR units are also sensitive to noise damage, which would coincide with the evidence of such a large reduction in electrophysiological responses despite the low-SR units contributing

only a small amount in the total number of ANFs. The reduction was so large that even the high-SR units may have been damaged as well.

We employed an AM signal at a relatively high level (80 dB SPL) to test the cochlear function at a suprathreshold level. We assume that the AM with a high modulation depth presents a large dynamic change of signal intensity, which challenge the ANFs with high-SRs with their small dynamic ranges, and require the response of ANFs with low-SRs that have large dynamic ranges. Therefore, one would expect to see more reduction in AM responses with higher modulation depths, since the low-SR ANFs are damaged by the noise (Furman, Kujawa, & Liberman, 2013; Song et al., 2016), especially when it is observed at suprathresold levels as in the present study (Figure 4). Although synapses innervating the medium and high-SR ANFs could also have been damaged as discussed above, the greater reduction in AM CAP amplitudes after noise exposure is more likely due to the damage and repair of low-SR ANF synapses.

When comparing the greater reduction of the AM CAP response compared to the click and tone burst CAP response, the differences in first spike latencies (FSLs) for different SR unit groups could be considered. Bourien et al. (2014) determined that the FSLs for low-SR units were delayed, but also more varied and therefore less synchronous. This difference would cause low-SR units to contribute less to the synchronous CAP response. However, at 100% modulation depth, the large change in amplitude should require ANFs with large dynamic ranges. This could indicate the need for low- and medium-SR units to be used to process the AM signals. Therefore, the greater reduction in the AM CAP response versus the CAP response alone may be a result of the more noise sensitive and therefore more damaged low-SR units. The AM

stimuli itself is also much longer in duration than the click and the simple tone burst. The AM stimuli then may include low-SR units since their FSLs are more delayed than higher-SR units. Therefore, for the AM stimuli, there could be a greater chance to include the low-SR units in the responses, but if they have been damaged more selectivity than higher-SR units, this would also show a greater reduction in the AM CAP response than the click or tone burst CAP.

We intended to obtain molecular evidence for the synaptic repair. However, we failed to obtain evidence at the translational level using Western blotting. There are several reasons for this including, poor antibodies, small concentration of proteins of interest and experimental error due to inexperience. These reasons will be discussed further below. At the transcription level, mRNA of the key ribbon protein, CtBP2 appears to be increased 1WPN (when using reference genes). However, the change does not reach statistical significance. A big limitation of this study is a combination of technique inexperience, resulting in large variations with replicates, and questionable reference genes used to analyze the data. The former reduces our ability to detect small relative differences and the latter brings our validity into question. Therefore, discussed below are the limitations of the reference genes.

Interestingly, a previous study found GAP43 protein to be up-regulated in guinea pigs after inner ear damage (Dodson & Mohuiddin, 2000). Our study found GAP43 mRNA to be down-regulated at 1 DPN. However differences do exist between the two studies. Their guinea pigs were given drugs to cause hair cell loss, while our guinea pigs were exposed to a noise level that have been previously found not to cause hair cell loss (Furman et al., 2013). Additionally, they monitored levels of GAP43 protein by

immunolabeling ganglion cells, where in this study RNA was extracted and studied by RT-qPCR methods. The drug study found up-regulation at three and six weeks post-drug exposure of the protein. One would expect that if more protein was generated, the mRNA concentration would also increase to produce this protein. However, these differences were not found in our guinea pigs with noise exposure, since the 1 MPN samples were similar to controls. The destruction of hair cells by drugs caused significant immediate damage which resulted in apoptosis of many nerve cells (Melgar–Rojas et al., 2015). The surviving neurons went through this apparent recovery phase with increased size and protein amounts for GAP43. While neuron damage has been reported with HHL noise exposure, it is usually over a longer time period (Furman et al., 2013; Kujawa & Liberman, 2009) and this could result in more subtle changes in GAP43 expression resulting in it being harder to detect or possibly occurring past 1 MPN. An incomplete recovery of synapses seem to occur within a month (Liu et al., 2012) for guinea pigs. However, perhaps the SGN damage is a much longer term as previously suggested and repair mechanisms of increased GAP43 are harder to detect without testing more time points. It is more difficult to give a reason as to explain the down-regulation from noise exposure after one day. A possible explanation could be that the lower amounts of GAP43 mRNA is a result of degradation after multiple translations to create more GAP43 protein 1 DPN. However, the lack of accurate Western Blot results means that this theory cannot be substantiated.

With research it is important to understand the underlying theories and limitations of the proposed methods one wishes to use. While the present contributions with the protein and mRNA analyses either failed completely or lacked statistical significance,

important groundwork has been laid for future research in this area when working with the cochlea of guinea pigs. Therefore, discussed below is a review of the limitations previously mentioned with regards to the Western Blotting and the RT-qPCR techniques.

4.1 Limitations of RT-qPCR

4.1.1 Reference Gene Validation

While RT-qPCR has made nucleic acid monitoring much easier, the lack of standardization of the technique has created a multitude of practices that have caused a large amount of data that may not be reproducible or accurate (Bustin et al., 2009; Taylor et al., 2010). The goal of Bustin et al., was to ensure that certain experimental steps were done to ensure the accuracy of these qPCR experiments to the Field (2009). One of these experimental steps necessary for proper research, is to include reference genes (formally known as house-keeping genes). Reference genes are used to standardize the genes of interest by accounting for differences in the starting amount of the cDNA template (for example after the reverse transcription step). The goal of a good reference gene is to be stable. This means that regardless of experimental condition, there should be little variability for the expression level of said reference gene.

Accordingly, reference genes have been previously used (Bustin et al., 2009). However, the original methodology was to use a single standard reference gene for all experiments. This concept is not feasible, since certain reference genes previously used may not be unaffected by the experimental conditions if they have never been tested specifically for the conditions in a new experiment. In fact, the correct number of reference genes to use is strongly recommended to be determined experimentally (Bustin

et al., 2009). However, for any analysis of reference gene stability, at least two reference genes are required.

Unfortunately, the overall criteria to determine if a reference gene is stable enough is not always apparent. There exists several software analysis systems to calculate the stability of a reference gene (Robledo et al., 2014; Spiegelaere et al., 2015). However, even after using an analysis program, the appropriate cut-off values for stability are not always stated. Here, four systems will be discussed briefly, both commercially available and available for free online.

Bio-Rad is a company that offers a qPCR detection system for sale, the CFX96 Touch™, along with its CFX Manager™ software program. According to its manual a stability 'M value' is calculated from taking your reference genes and testing a subset or all samples with primers for your reference genes. It states that an 'M value' of less than 0.5 is required for homogenous samples or less than 1.0 for heterogeneous samples. Homogenous samples refer to samples of the same cell type where heterogeneous is when samples contain multiple sample types. Interestingly, using this software, one can analyze that data by looking at samples individually, or by grouping them together by experimental condition (e.g. control versus noise exposure of different time points). The software gives two different 'M values' depending on what analysis option you choose, however the same cut-off values are still suggested (less than 0.5 or less than 1.0 depending on samples). By providing two different analyses options, each with their own different stability 'M values' for reference genes, this suggests that if you want to analyze the data you have to meet the criteria through at least one analysis pathway option. Therefore one would have to use that particular option to further analyze data if

they meet criteria. However, other methods of analyses do exist, as previously mentioned.

For example, NormFinder is a free excel spreadsheet program provided by the Molecular Diagnostic Laboratory at Aarhus University Hospital Skejby, in Denmark (Andersen et al., 2004). This software takes into account the individual samples as well as the experimental groups (conditions) that are a part of using the relative quantity data. It provides a stability value for individual reference genes and then selects the best two reference genes to be used together, while also providing a stability value for the two best reference genes it selected. Additionally, it gives the statistics on intra and inter group variability, which is desirable to be as low as possible. However, unlike Bio-Rad's software, no cut-off stability value is given for NormFinder, except for the similar concept that the lower the stability value is, the more stable it is to use as a reference gene.

Additionally, another free excel spreadsheet analysis software for reference genes is BestKeeper (Pfaffl et al., 2004). This system provides a multitude of statistics, however, the only apparent cut-off that people use is the calculated standard deviation value (SD) for each reference gene. To be accepted as a reference gene, the SD must be below 1.0. Another criteria suggested to use in the software is the coefficient of variation (CV). Once again, no apparent cut-off value is given for CV, however it is understood that the lower the value, the more stable the reference gene.

Finally, there is also GeNorm, a commercially based software (Vandesompele et al., 2002). This software also generates a statistical 'M value' for reference gene stability. Its relation to the 'M value' determined by Bio-Rad's CFX Manager™ is not

certain at the time of writing this thesis. However, current published articles appear to use the criteria of GeNorm's cut-off value for the 'M value' to be 1.5 (Kaluzna, Kuras, & Pulawska, 2017; Petriccione, Mastrobuoni, Zampella, & Scortichini, 2015; Wang, Zhang, Liu, Liu, & Ding, 2017).

Interestingly, it appears that current published articles still use multiple programs to determine the most stable genes to use as reference genes (Kaluzna et al., 2017; Melgar–Rojas et al., 2015; Petriccione et al., 2015; Robledo et al., 2014; Spiegelaere et al., 2015; Wang et al., 2017). Discrepancies between the different software show that different methods of determining stability do not always give similar results (Kaluzna et al., 2017). Therefore, it appears to be useful to cross-check between different methodologies and to create a ranking table of stability values to determine the most stable reference genes. However, the lack of cut-off values for some of these methods cause ambiguity and may result in choosing the best reference genes out of all the ones being tested. But, that doesn't necessarily mean that they are stable enough to use, just stable out of all being tested. When designing an RT-qPCR experiment, it is important to look at these many validation steps that are required to generate evidence to support one's conclusions from the data.

Using free applications, several factors of stability were found for each of the remaining three potential reference genes tested in this study (Table 4). With the lower the value being an indication of improved stability, it was found that the gene Rplp0 was found the most stable of the three tested. Hprt1 was ranked second two out of three times, making it next best reference gene of the ones tested. This philosophy of having

no exact cut-off value for these software indicating stability causes some concerns especially when testing only a few reference genes as in this study.

Table 4. Free software analyses of reference gene stability.

Rank	BestKeeper (SD)	BestKeeper (CV%)	Normfinder
1	RPLP0 (0.64)	RPLP0 (2.10)	RPLP0 (0.179)
2	B2M (0.80)	HPRT1 (3.02)	HPRT1 (0.299)
3	HPRT1 (0.92)	B2M (3.25)	B2M (0.305)

Consequently, the desire to look at other software arose when Bio-Rad's CFX Manager Software that was used to collect the data gave interesting results of gene stability (Table 5). These stability factors were lowest for using Hprt1 and Rplp0 as reference genes. Bio-Rad's software provided a stability 'M' value differently if the samples were grouped or analyzed separately, however listed the same cut-off values for both, described earlier (Taylor et al., 2010). Depending on what option to analyze data one chooses, a differing conclusion of stability could be drawn. These cut-off values indicate proper reference gene stability for homogenous samples (same cell type) for an 'M' stability factor of less than 0.5 and for heterogeneous samples (different cells, ie. tissue) of less than 1.0. The samples for this study were entire cochleae which makes it heterogeneous. While technically in this case both stability values fall under this cut-off value, the individual stability factor is approaching 0.9135. This value was obtained using only a subset of the samples, therefore all samples were tested next, which found some improvement in overall stability for the individual and grouped analyses.

Table 5. Bio-Rad's CFX Manager Software analysis of reference gene stability.

	Subset of Samples 'M' Stability Factor		Full Samples 'M' Stability Factor	
Optimal Reference Combination	Individual	Grouped	Individual	Grouped
	0.9135	0.1887	0.8094	0.1681

Regardless, the individual stability factor is still quite high, though within previously published cut-off values (Taylor et al., 2010). From this study it is surmised that the grouped analysis of stability is a more general stability assessment, but for stricter analysis the individual samples should be looked at. Reference genes are supposed to be similarly expressed regardless of sample or condition (Bustin et al., 2009; Taylor et al., 2010). This concept is used to adjust the genes of interest to account for variations in pipetting and the reverse transcription reaction. Therefore, since individual samples would each have their own variation, it would make sense to look at stability at the individual sample level as a better indicator of stability than group. However, other software, like NormFinder, takes into account the groups the sample is in (Andersen et al., 2004). Perhaps the best way is to look at both group and individual stability. Having looked at the numerical stability determination, one can also look at it visually (Figure 9).

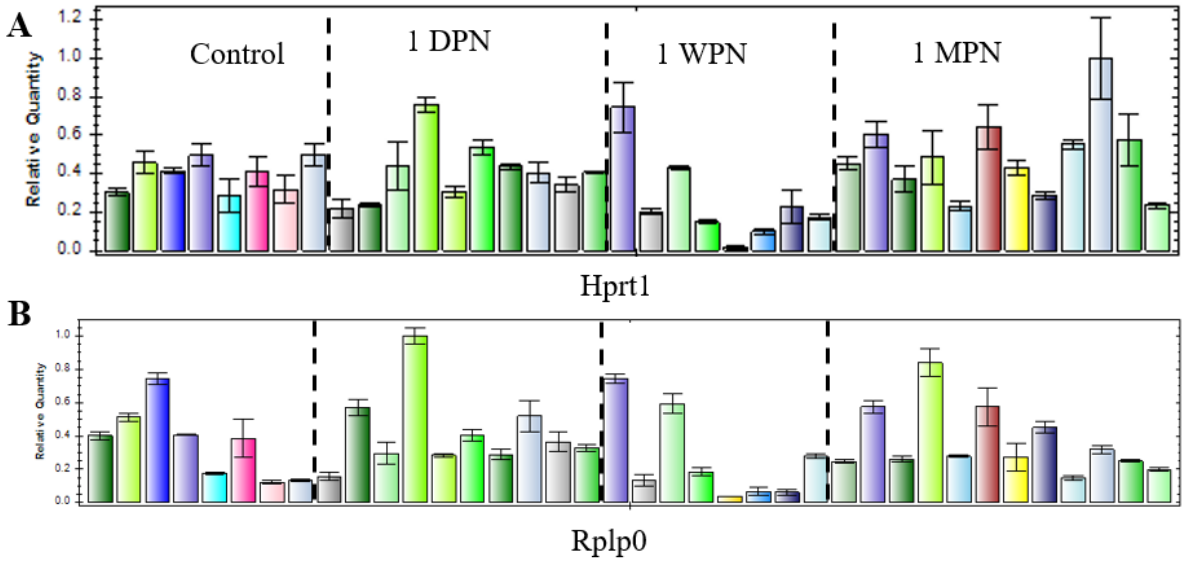

Figure 9. Reference Gene comparison of expression for individual samples. (A) Hprt1 and (B) Rplp0 (+/- 1 Standard error of the mean, SEM).

As described previously, one would imagine that a good reference gene would be equally expressed with minimal variation across each sample. However, for both potential reference genes, Hprt1 and Rplp0, this does not appear to be the case. Some samples are more highly expressed than others when looking at each reference gene separately. But, even though this variability is present, the goal of a reference gene is to account for pipetting variations. Therefore, it is possible that the variability is caused by these variations. The question that remains is how does one determine a gene's stability? It is by having at least two reference genes to test with (Taylor et al., 2010). Even if one reference gene varies across samples, if another reference gene varies in a similar manner across the same samples, then those reference genes are stable and effective. The logic follows that the more genes one tests that follows the same variations, the more confident

one is in assuming that those variations are purely due to pipetting differences and not for different gene expressions.

Accordingly, comparing both Figure 9A and 9B visually there are similar trends in variation across the same samples. The lowly expressed 1 WPN group, when compared to other samples in other groups, have a similar pattern present for both Hprt1 and Rplp0. But, not all of the samples appear to follow their counterpart between the two reference genes. While this visual inspection is not an effective means of determining stability it can provide reinforcement in confidence in the obtained stability values.

Returning to the free software analyses (Table 4), the study that these reference genes were obtained from looked at these programs as well (Melgar–Rojas et al., 2015). The values found from the literature are much lower, and therefore considered more stable, than obtained in this study (Table 6). However, it should be pointed out that this study looked at noise exposure in rats, while this research looks at guinea pigs. This discrepancy could be related to species. However, Melgar–Rojas et al. had used only 23 rats, while 37 guinea pigs were tested here (2015). One would imagine that the higher sample size would not show such variability, if they were good reference genes for guinea pigs.

Table 6. Reference gene stability comparison with the literature.

Stability Factor	Results found in this study		Results found by (Melgar–Rojas et al., 2015)	
	Rplp0	Hprt1	Rplp0	Hprt1
BestKeeper (SD)	0.64	0.92	0.23	0.23
BestKeeper (CV%)	2.10	3.02	1.32	1.05
NormFinder	0.179	0.299	~0.075	~0.085

Overall, the stability of these reference genes is questionable based on the large variability they present across samples with a single reference gene, though some trends across samples between reference genes are present. Additionally, for both group and individual analyses of stability with Bio-Rad's software, the genes do fall under the stability cut-off, though just barely with individual samples. For these reasons the confidence in using these reference genes to further analyze the genes of interest is uncertain. Therefore, genes of interest were analyzed with and without reference genes, though the latter is not normal practice. This was done to compare how the results change.

4.1.2 Genes of Interest Analysis

The limitations of the genes should be noted. For example, the Ctbp2 primer will detect both Ribeye (B domain) ribbon synapse and Ctbp2 nucleic genes. The specific Ribeye A domain DNA sequence was not found when designing primers. So the goal was to use Ctbp2 primers and to compare it with other genes associated with the ribbon

synapse. Bassoon was found to have multiple peaks in some of the melt curves, indicating non-specific amplification. Additionally, the no-template control (NTC) had a response for Bassoon indicating genomic DNA contamination (Figure 10). Steps were taken to remove genomic DNA, since we only want to amplify cDNA from the converted RNA step. Perhaps since Bassoon is such a large sequence, it may have been more difficult to fully degrade its genomic DNA. Regardless, this means that Bassoon cannot be reliably quantified because we can't distinguish the response between the genomic DNA and the cDNA. Luckily, no other contamination of reagents or genomic DNA was found for the other primers (Figure A6).

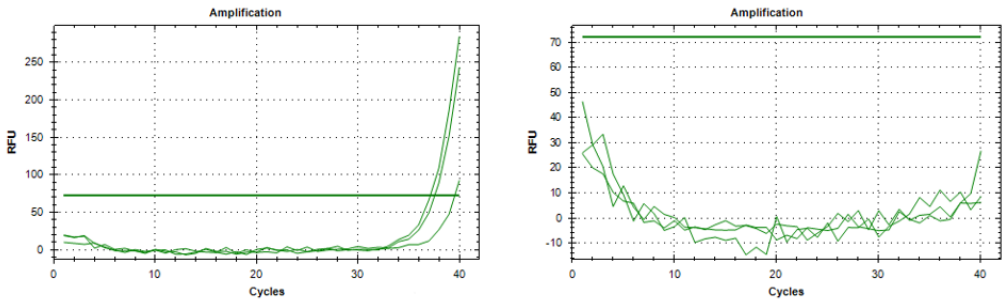

Figure 10. NRT and NTC checks for Bassoon.

Even though significant changes were not found certain trends can be seen visually (Figure 7). When comparing each analysis (with and without reference genes), the biggest difference between the two is the 1 WPN group. This makes sense, since both reference genes showed lower expression for the 1 WPN group compared to other samples (Figure 9). Therefore, the 1 WPN group would be subject to greater adjustment when using reference genes as opposed to not using them. This is a good example of

how potentially poor reference genes can skew the final result. Whether or not the reference genes used here are adequate is uncertain as discussed previously.

But, what the analysis with the reference gene suggests is that there is a trend of up-regulation for Bassoon (which we cannot reliably use now), Ctbp2 and Rim2 at the 1 WPN time point. This is interesting because previous research has found repair, albeit incomplete, of the ribbon synapse at around one month (Liu et al., 2012; Shi et al., 2013; Song et al., 2016). To see higher expression of mRNA at around 1 WPN would indicate potential repair of the synapses by the one month timeline. However, these trends disappear when no reference genes are used.

4.2 Limitations of Western Blotting

4.2.1 Reliable Detection Issues

As previously mentioned, Western Blotting was done to analyze the harvested proteins. However, while this technique has been around for decades, to ensure proper validity and reliability, proper steps must be taken to standardize this testing (Gilda & Gomes, 2013; Taylor et al., 2013; Taylor & Posch, 2014). Firstly, to normalize each sample, one of two possible methods must be utilized. Originally, a house-keeping protein was used to normalize the gel/membrane. House-keeping proteins are proteins whose concentration is stable regardless of experimental condition (Taylor & Posch, 2014). However, house-keeping proteins tend to be highly expressed in individual samples and there is an increased risk of oversaturating the gel/membrane with unwanted protein to detect the potentially much smaller amount of protein of interest. Therefore, the other possible method that has been found to be more useful is total lane normalization (Gilda & Gomes, 2013; Taylor et al., 2013). Total lane normalization requires the use of a special stain that is present throughout the pre-run gel. Upon activation with UV light, the stain highlights all protein. The intensity of this signal from a control lane on the membrane can then be used to normalize the antibody detection signal data. Secondly, as determined by a protein assay, the amount of total protein to be loaded onto each gel lane must be determined by finding the linear region. Therefore, any plateau effects would be avoided. If these steps are taken into consideration, Western Blotting can be used to determine relative protein amounts.

As discussed earlier, Ribeye, the protein that makes up the ribbon, has two domains (A and B) (Schmitz et al., 2000; Uthaiah & Hudspeth, 2010). The B domain is

essentially the sequence of another protein, Ctbp2, minus 20 amino acids. Previous research and shown that when using Ctbp2 antibodies you can detect both Ctbp2 and Ribeye (through the B domain). Therefore, while the Ctbp2 antibody did detect a band, it only detected it at 47 kDa, which is consistent for Ctbp2 the transcription repressor and not Ribeye through the B domain (Table 7). This work through pooled samples showed no detectable Ribeye. However, to see if any detectable Ribeye was found with individual samples, the Ctbp2 antibody was continued to be used.

Table 7. Molecular size of proteins that were detectable. [1]Ctbp2, the transcription repressor, is much smaller than Ribeye and contains a B domain that is the same as Ctbp2 (Uthaiah & Hudspeth, 2010). [2]GAP43 has been found to have a variable detectable size when doing SDS-PAGE (Sigma-Aldrich, 2014).

Molecular Size (kDa)	Protein		
	Ctbp2	Ribeye	GAP43
Theoretical[1,2]	~50	120	43-57
Detected	48	-	55

There are many reasons why many of the proteins of interest were not detectable. First of all, experimental error could be the cause since many steps are involved in Western blotting. Additionally, the antibodies themselves may not be effective. All the antibodies used were not rated experimentally by the manufacture to be used on guinea pigs, but for other smaller mammals like rats, mice and hamsters. Antibodies for these proteins that have been used on guinea pigs for western blotting were not found. Also, the proteins themselves could be tricky to detect. For example, Bassoon is a large protein

of > 420 kDa in size (Jing et al., 2013). Large proteins are harder to transfer from the gel to the membrane. Trying different membrane materials with different transfer protocols can be used to detect difficult proteins, however, all attempts failed. Finally, the ribbon synapses are known to have low concentrations in the hair cells of animals such as mice and chickens (Uthaiah & Hudspeth, 2010). Therefore, it is possible that they are in such low concentration per cochlea of a guinea pig, that Western Blotting relative quantitation techniques are not sufficient to use.

Of the detected bands, it is noted that the membrane western blot images for Gap43 (Figure 11) and Ctbp2 (Figure 12) have a large background signal that creates an uneven blotting image. Additionally, the collection time of the image was quite long, indicating that the signal was very low. Whether this is due to natural low quantity of Ctbp2 (transcription repressor) and Gap43 or if protein harvesting procedures were poor, this is unknown. However, the result is that with these poor western blot images, bands will be harder to detect reliably.

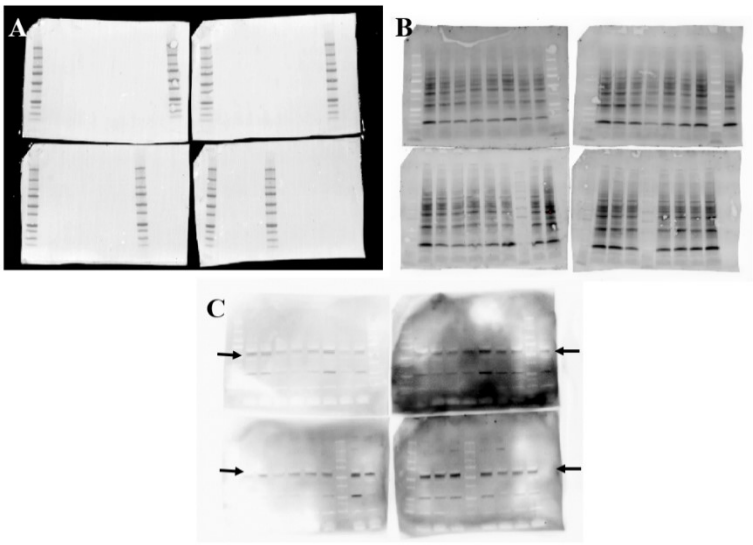

Figure 11. ChemiDoc™ images for GAP43 protein. (A) Colourmetric image of protein ladder to verify the size of the protein of interest. (B) Stain-Free™ image of total protein used to normalize data. (C) Blotting image of GAP43 antibody, with arrows indicating the band of interest.

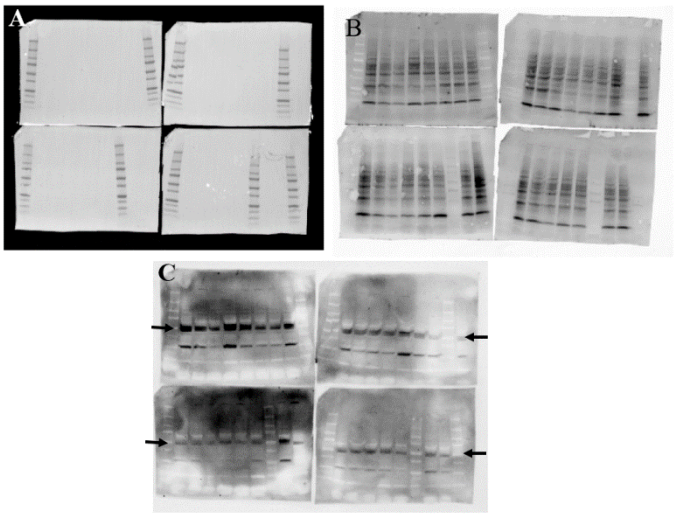

Figure 12. ChemiDoc™ images for Ctbp2 protein. (A) Colourmetric image of protein ladder to verify the size of the protein of interest. (B) Stain-Free™ image of total protein used to normalize data. (C) Blotting image of Ctbp2 antibody, with arrows indicating the band of interest.

It is important to remember the scale that we are working with. The total protein loaded comprises the more common proteins of an entire cochlea, compared to the much lower concentration of synaptic proteins. Therefore, future harvesting may be better to do with more selective tissue extraction. The downside of doing this, is that more time will be spent harvesting, which gives proteins more time to degrade.

4.2.2 Protein Loading Linear Range Detection

To ensure the proper amount of total protein is loaded from each sample onto the gel, a linear region must be found for each protein (Taylor & Posch, 2014). This allows for the determination that if no significant protein changes are found, than it is because the cochlea themselves did not produce varying amounts of the protein. Otherwise, if not done, the detection of that protein could be within a plateau. The latter statement tells us nothing since if we load in a plateau, detectable amounts are not quantifiable if no significant change is found. Unfortunately, the experiment for the linear range failed to give reliable results. The previously mentioned background issue with blotting caused the bands to be difficult to detect (Figure 13). One should be looking at a series of bands that at first are quite dark (more total protein loaded) then get lighter and lighter until it can not be detected. However, every time the experiment was run for the linear range, the intensities did not follow expectation.

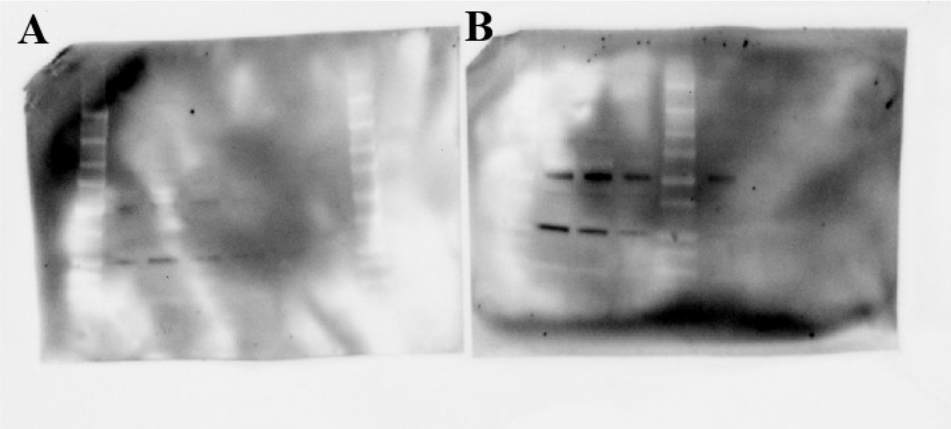

Figure 13. ChemiDoc™ membrane images of linear range of loading amount for (A) Ctbp2 and (B) GAP43.

For example, Gap43 should have shown increasing intensity for the increasing amount of protein loaded. However, the opposite was found for one test if one data point was removed (Figure 14). Recall that this experiment was done with a pooled sample. To determine that if any significant differences occur between groups, the experiments with Western Blotting were continued, even though no linear range of loading sample was determined. This was done understanding the limitations of interpreting the obtained results. To continue, 40 µg of total protein to load was selected based on the desire to not overload the gel/membrane with protein but to hopefully have enough to detect significant differences between the groups. The randomness of selecting this amount drives the understanding of how important it is to properly determine the loading amount. The possible reasons resulting in the failure of finding the linear region are similar to those previously mentioned.

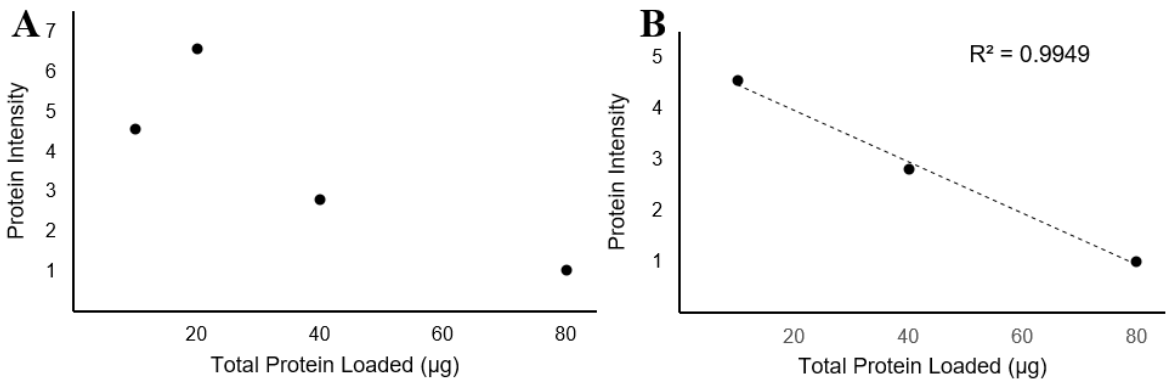

Figure 14. Normalized fold difference protein expression of pooled sample's loading amount linear range for GAP43. **(A)** All detected bands. **(B)** Single data point of 20 µg removed to show linearity, but inversely related and thus opposite than expected.

Therefore the Western Blot results (Figure 8) of finding no significance is meaningless because a linear range was not found for the total loaded proteins. Only if a significant difference was found, would a result tell us something with regards to noise exposure with these proteins.

The Ctbp2 results obtained were only for the transcription repressor and not the desired Ribeye (B domain). No bands around 120 kDa was detected. Therefore, even if the Western blot results were usable for Ctbp2, it would be for the wrong protein.

Chapter 5 Conclusion

Overall, no strong molecular evidence was seen for ribbon synaptic repair in the guinea pig NIHHL model from the Western and PCR data obtained in this study. Protein analysis failed due to lack of detection and/or the ability to determine the loading linear range of the total protein for the gel. This could be the result of the expected low amount of protein relative to the entire cochlea proteome. Further research into this area will require testing more antibodies, but also finding methods to quickly, but more selectively, harvest hair cells. This would hopefully improve the signal-to-noise ratio of proteins of interest to total protein collected.

Additionally, the results from the RNA analysis are suspect for validity since the reference genes just barely meet criteria. However, several different analyses found no significant differences besides a down-regulation of GAP43 at the 1 DPN time point, which is a potentially odd finding based on an ototoxicity model previously found (Dodson & Mohuiddin, 2000). Although certain trends of up-regulation are apparent at the 1 WPN when using the reference gene analysis for the synaptic proteins, there is an insufficient difference to suggest a significant change for ribbon synaptic repair. To improve this, more reference genes should be tested to have better confirmation of pipetting differences between samples. However, this uncertainty around the reference genes and how to determine their stability, highlights the Field's need to continue to develop better standards that everyone should follow. Interestingly, many of the primers tested here were newly developed and were based on mostly theoretical guinea pig DNA. Stability aside, both the primers for reference genes and genes of interest, excluding

Bassoon and Tbp, have shown to be effective for cochlear guinea pig samples. Therefore, these primers can be utilized for future research with guinea pigs.

Functional tests indicated no permanent threshold shifts for these guinea pigs, however CAP responses did not fully recover after 1 MPN and AM response deficits at suprathreshold levels, especially at high modulation depths, were found. Further testing using AM signals at lower sound levels should be done to further explore the potential impact on high-SR ANFs.

HHL is a phenomenon that has been found in smaller mammals and could explain hearing difficulties in background noise for people who have not experienced significant permanent threshold changes (Kujawa & Liberman, 2009; Song et al., 2016). No repair was found in mouse models, while repair may be happening in guinea pigs. Continued research into HHL is important to fully understand the mechanism of it. Once it is better understood, measures can be taken to improve the limitations HHL imposes on temporal auditory processing.

References

Albuquerque, A. A. S., Rossato, M., Oliveira, J. A. A. De, & Hyppolito, M. A. (2009). Understanding the anatomy of ears from guinea pigs and rats and its use in basic otologic research. *Brazilian Journal of Otorhinolaryngology*, *75*(1), 43–49.

Andersen, C. L., Jensen, J. L., & Ørntoft, T. F. (2004). Normalization of Real-Time Quantitative Reverse Transcription-PCR Data : A Model-Based Variance Estimation Approach to Identify Genes Suited for Normalization , Applied to Bladder and Colon Cancer Data Sets. *Cancer Research*, *64*, 5245–5250.

Bharadwaj, H. M., Masud, S., Mehraei, G., Verhulst, S., & Shinn-Cunningham, B. G. (2015). Individual differences reveal correlates of hidden hearing deficits. *Journal of Neuroscience*, *35*(5), 2161–2172. http://doi.org/10.1523/JNEUROSCI.3915-14.2015

Bourien, J., Tang, Y., Batrel, C., Huet, A., Lenoir, M., Ladrech, S., … Wang, J. (2014). Contribution of auditory nerve fibers to compound action potential of the auditory nerve. *Journal of Neurophysiology*, *112*(5), 1025–1039. http://doi.org/10.1152/jn.00738.2013

Bramhall, N. F., Konrad-Martin, D., McMillan, G. P., & Griest, S. E. (2017). Auditory Brainstem Response Altered in Humans with Noise Exposure Despite Normal Outer Hair Cell Function. *Ear and Hearing*, *38*(1), 1–27. http://doi.org/10.1097/AUD.0000000000000370.Auditory

Buran, B. N., Strenzke, N., Neef, A., Gundelfinger, E. D., Moser, T., & Liberman, M. C. (2010). Onset coding is degraded in auditory nerve fibers from mutant mice lacking synaptic ribbons. *Journal of Neuroscience*, *30*(22), 7587–7597. http://doi.org/10.1523/JNEUROSCI.0389-10.2010

Bustin, S. A., Benes, V., Garson, J. A., Hellemans, J., Huggett, J., Kubista, M., … Wittwer, C. T. (2009). The MIQE guidelines: minimum information for publication of quantitative real-time PCR experiments. *Clinical Chemistry*, *55*(4), 611–622. http://doi.org/10.1373/clinchem.2008.112797

Dodson, H. C., & Mohuiddin, A. (2000). Response of spiral ganglion neurones to cochlear hair cell destruction in the guinea pig. *Journal of Neurocytology*, *29*(7), 525–537. http://doi.org/10.1023/A:1007201913730

Furman, A. C., Kujawa, S. G., & Liberman, M. C. (2013). Noise-induced cochlear neuropathy is selective for fibers with low spontaneous rates. *Journal of Neurophysiology*, *110*(3), 577–586. http://doi.org/10.1152/jn.00164.2013

Gebhart, M., Juhasz-Vedres, G., Zuccotti, A., Brandt, N., Engel, J., Trockenbacher, A., … Striessnig, J. (2010). Modulation of Cav1.3 Ca2+ channel gating by Rab3 interacting molecule. *Molecular and Cellular Neuroscience*, *44*(3), 246–259. http://doi.org/10.1016/j.mcn.2010.03.011

Gelfand, S. A. (2010). *Hearing: An introduction to psychological and physiological acoustics (5th ed.)*. New York, NY: informa Healthcare.

Gilda, J. E., & Gomes, A. V. (2013). Stain-free total protein staining is a superior loading control to β-actin for Western Blots. *Analytical Biochemistry*, *440*(2), 186–188. http://doi.org/10.1016/j.ab.2013.05.027

Glowatzki, E., & Fuchs, P. A. (2002). Transmitter release at the hair cell ribbon synapse. *Nature Neuroscience*, *5*(2), 147–154. http://doi.org/10.1038/nn796

Goni, R., García, P., & Foissac, S. (2009). The qPCR data statistical analysis. *Integromics White Paper*, 1–9. Retrieved from http://www.gene-quantification.eu/integromics-qpcr-statistics-white-paper.pdf

Haynes W. O. & Johnson, C. E. (2009). Understanding Research and Evidence-Based Practice in Communication Disorders: A Primer for Students and Practitioners. Toronto: Pearson.

Health Canada (2016). *Noise induced hearing loss; It's your health* (Catalogue # H13-7/128-2012E-PDF). Retrieved from https://www.canada.ca/en/health-canada/services/healthy-living/your-health/environment/noise-induced-hearing-loss.html

Heil, P., & Peterson, A. J. (2015). Basic response properties of auditory nerve fibers: a review. *Cell and Tissue Research*, *361*(1), 129–158. http://doi.org/10.1007/s00441-015-2177-9

Hind, S. E., Haines-Bazrafshan, R., Benton, C. L., Brassington, W., Towle, B., & Moore, D. R. (2011). Prevalence of clinical referrals having hearing thresholds within normal limits. *International Journal of Audiology*, *50*(10), 708–716. http://doi.org/10.3109/14992027.2011.582049

Jing, Z., Rutherford, M. A., Takago, H., Frank, T., Fejtova, A., Khimich, D., … Strenzke, N. (2013). Disruption of the presynaptic cytomatrix protein bassoon degrades ribbon anchorage, multiquantal release, and sound encoding at the hair cell afferent synapse. *Journal of Neuroscience*, *33*(10), 4456–4467. http://doi.org/10.1523/JNEUROSCI.3491-12.2013

Jung, S., Oshima-Takago, T., Chakrabarti, R., Wong, A. B., Jing, Z., Yamanbaeva, G., … Moser, T. (2015). Rab3-interacting molecules 2alpha and 2beta promote the abundance of voltage-gated CaV1.3 Ca2+ channels at hair cell active zones. *Proceedings of the National Academy of Sciences of the United States of America*, *112*(24), E3141-9. http://doi.org/10.1073/pnas.1417207112

Kaluzna, M., Kuras, A., & Pulawska, J. (2017). Validation of reference genes for the normalization of the RT-qPCR gene expression of virulence genes of Erwinia amylovora in apple shoots. *Scientific Reports*, *7*, 1–9. http://doi.org/10.1038/s41598-017-02078-4

Khimich, D., Nouvian, R., Pujol, R., tom Dieck, S., Egner, A., Gundelfinger, E. D., & Moser, T. (2005). Hair cell synaptic ribbons are essential for synchronous auditory signalling. *Nature*, *434*(7035), 889–894. http://doi.org/10.1038/nature03418

Koressaar T, Remm M (2007) Enhancements and modifications of primer design program Primer3 *Bioinformatics 23*(10), 1289-91

Kramer, S.; Jerger, J. & Mueller, G. H. (2014). Audiology: Science to Practice (2nd ed). San Diego, CA; Plural Publishing.

Kujawa, S. G., & Liberman, M. C. (2009). Adding Insult to Injury: Cochlear Nerve Degeneration after "Temporary" Noise-Induced Hearing Loss. *Journal of Neuroscience*, *29*(45), 14077–14085. http://doi.org/10.1523/JNEUROSCI.2845-09.2009

Liberman, L. D., Wang, H., & Liberman, M. C. (2011). Opposing gradients of ribbon size and AMPA receptor expression underlie sensitivity differences among cochlear-nerve/hair-cell synapses. *Journal of Neuroscience*, *31*(3), 801–808. http://doi.org/10.1523/JNEUROSCI.3389-10.2011

Liberman M. C., (1978). Auditory-nerve response from cats raised in a low-noise chamber. *Journal of the Acoustical Society of America*, *63*(2), 442-55.

Liberman, M. C. (1982). Single-Neuron Labeling in the Cat Auditory Nerve. *Science*, *216*, 1239–1241.

Liberman, M. C., Epstein, M. J., Cleveland, S. S., Wang, H., & Maison, S. F. (2016). Toward a differential diagnosis of hidden hearing loss in humans. *PLoS ONE*, *11*(9), 1–15. http://doi.org/10.1371/journal.pone.0162726

Liu, L., Wang, H., Shi, L., Almuklass, A., He, T., Aiken, S., … Wang, J. (2012). Silent damage of noise on cochlear afferent innervation in guinea pigs and the impact on temporal processing. *PLoS ONE*, *7*(11), 1–11. http://doi.org/10.1371/journal.pone.0049550

Lobarinas, E., Spankovich, C., & Le Prell, C. G. (2016). Evidence of "hidden hearing loss" following noise exposures that produce robust TTS and ABR wave-I amplitude reductions. *Hearing Research*, *349*, 155–163. http://doi.org/10.1016/j.heares.2016.12.009

Mehraei, G., Hickox, A. E., Bharadwaj, H. M., Goldberg, H., Verhulst, S., Liberman, M. C., & Shinn-Cunningham, B. G. (2016). Auditory Brainstem Response Latency in Noise as a Marker of Cochlear Synaptopathy. *The Journal of Neuroscience*, *36*(13), 3755–3764. http://doi.org/10.1523/JNEUROSCI.4460-15.2016

Melgar–Rojas, P., Alvarado, J. C., Fuentes–Santamaría, V., Gabaldón–Ull, M. C., & Juiz, J. M. (2015). Validation of reference genes for RT–qPCR analysis in noise–induced hearing loss: A study in Wistar rat. *PLoS ONE*, *10*(9), 1–25. http://doi.org/10.1371/journal.pone.0138027

Merchan-Perez, A., & Liberman, M. C. (1996). Ultrastructural differences among afferent synapses on cochlear hair cells: Correlations with spontaneous discharge rate. *Journal of Comparative Neurology*, *371*(2), 208–221. http://doi.org/10.1002/(SICI)1096-9861(19960722)371:2<208::AID-CNE2>3.3.CO;2-P

Moser, T., Brandt, A., & Lysakowski, A. (2006). Hair cell ribbon synapses. *Cell and Tissue Research*, *326*(2), 347–359. http://doi.org/10.1007/s00441-006-0276-3

Neitzel, R. L., Swinburn, T. K., Hammer, M. S., & Eisenberg, D. (2016). Economic Impact of Hearing Loss and Reduction of Noise-Induced Hearing Loss in the United States. *Journal of Speech, Language, and Hearing Research*, *60*, 182–189.

Petriccione, M., Mastrobuoni, F., Zampella, L., & Scortichini, M. (2015). Reference gene selection for normalization of RT-qPCR gene expression data from Actinidia deliciosa leaves infected with Pseudomonas syringae pv . actinidiae. *Nature Publishing Group*, *5*, 1–12. Retrieved from http://dx.doi.org/10.1038/srep16961

Pfaffl, M. W., Tichopad, A., Prgomet, C., & Neuvians, T. P. (2004). Determination of stable housekeeping genes , differentially regulated target genes and sample integrity : BestKeeper – Excel-based tool using pair-wise correlations. *Biotechnology Letters*, *26*, 509–515.

Plack, C. J., Barker, D., & Prendergast, G. (2014). Perceptual Consequences of "Hidden" Hearing Loss. *Trends in Hearing*, *18*, 1–11. http://doi.org/10.1177/2331216514550621

Robledo, D., Hernández-Urcera, J., Cal, R. M., Pardo, B. G., Sánchez, L., Martínez, P., & Viñas, A. (2014). Analysis of qPCR reference gene stability determination methods and a practical approach for efficiency calculation on a turbot (Scophthalmus maximus) gonad dataset. *BMC Genomics*, *15*(1), 648. http://doi.org/10.1186/1471-2164-15-648

Safieddine, S., El-Amraoui, A., & Petit, C. (2012). The auditory hair cell ribbon synapse: from assembly to function. *Annual Review of Neuroscience*, *35*(1), 509–528. http://doi.org/10.1146/annurev-neuro-061010-113705

Schmitz, F., Königstorfer, A., & Südhof, T. C. (2000). RIBEYE, a component of synaptic ribbons. *Neuron*, *28*(3), 857–872. http://doi.org/10.1016/S0896-6273(00)00159-8

Shaw, G. (2017). NOISE-INDUCED HEARING LOSS: What your Patients don't know can hurt them. *The Hearing Journal*, *70*(5), 26–28. Retrieved from http://archotol.jamanetwork.com/article.aspx?articleid=587677

Shi, L., Liu, L., He, T., Guo, X., Yu, Z., Yin, S., & Wang, J. (2013). Ribbon synapse plasticity in the cochleae of guinea pigs after noise-induced silent damage. *PLoS ONE*, *8*(12), 1–9. http://doi.org/10.1371/journal.pone.0081566

Sigma-Aldrich, (2014). Monoclonal Anti-Growth Associated Protein-43 clone GAP-7B10 produced in mouse, ascites fluid. Retrieved from: http://www.sigmaaldrich.com/content/dam/sigma-aldrich/docs/Sigma/Datasheet/7/g9264dat.pdf

Song, Q., Shen, P., Li, X., Shi, L., Liu, L., Wang, J. J., … Wang, J. J. (2016). Coding deficits in hidden hearing loss induced by noise: the nature and impacts. *Scientific Reports*, *6*(April), 25200. http://doi.org/10.1038/srep25200

Spiegelaere, W. De, Dern-wieloch, J., Weigel, R., Schumacher, V., Vandekerckhove, L., & Fink, C. (2015). Reference Gene Validation for RT-qPCR , a Note on Different Available Software Packages. *PLos One*, *10*(3), 1–13.

Statistics Canada (2016). *Hearing loss of Canadians, 2012 to 2015.* Retrieved from http://www.statcan.gc.ca/pub/82-625-x/2016001/article/14658-eng.htm

Sterling, P., & Matthews, G. (2005). Structure and function of ribbon synapses. *Trends in Neurosciences*, *28*(1), 20–29. http://doi.org/10.1016/j.tins.2004.11.009

Taylor, S. C. (2016). *qPCR Training Series* [PowerPoint Slides]. Sir Charles Tupper Medical Building, Dalhousie University, Halifax, NS.

Taylor, S. C., Berkelman, T., Yadav, G., & Hammond, M. (2013). A defined methodology for reliable quantification of Western Blot data. *Molecular Biotechnology*, *55*(3), 217–226. http://doi.org/10.1007/s12033-013-9672-6

Taylor, S. C., & Posch, A. (2014). The design of a quantitative Western Blot experiment. *BioMed Research International*, 1–8. http://doi.org/10.1155/2014/361590

Taylor, S., Wakem, M., Dijkman, G., Alsarraj, M., & Nguyen, M. (2010). A practical approach to RT-qPCR—publishing data that conform to the MIQE guidelines. *Methods*, *50*(4), S1–S5. http://doi.org/10.1016/j.ymeth.2010.01.005

Untergasser A., Cutcutache I., Koressaar T., Ye J., Faircloth B.C., Remm M., Rozen S.G. (2012) Primer3 - new capabilities and interfaces. *Nucleic Acids Research* 40(15):e115

US National Library of Medicine (2017a). National Center of Biotechnology Information. Retrieved from https://www.ncbi.nlm.nih.gov/

US National Library of Medicine (2017b). National Center of Biotechnology Information Primer-Blast. Retrieved from https://www.ncbi.nlm.nih.gov/tools/primerblast/index.cgi?LINK_LOC=BlastDescAd

Uthaiah, R. C., & Hudspeth, A. J. (2010). Molecular anatomy of the hair cell's ribbon synapse. *Journal of Neuroscience*, *30*(37), 12387–12399. http://doi.org/10.1523/JNEUROSCI.1014-10.2010

Vandesompele, J., Preter, K. De, Poppe, B., Roy, N. Van, Paepe, A. De, & Speleman, F. (2002). Accurate normalization of real-time quantitative RT -PCR data by geometric averaging of multiple internal control genes. *Genome Biology*, *3*(7), 1–12.

Wang, H., Zhang, X., Liu, Q., Liu, X., & Ding, S. (2017). Selection and evaluation of new reference genes for RT-qPCR analysis in Epinephelus akaara based on transcriptome data. *PLos ONE*, *12*(2), 1–18.

Yuan, J., Reed, A., Chen, F., & Stewart, C. N. (2006). Statistical analysis of real-time PCR data. *BMC Bioinformatics*, *7*, 1–12. http://doi.org/10.1186/1471-2105-7-85

Appendix

7.1 Western Blotting

When testing for possible interference from the RIPA buffer when doing the protein assay, it was found that the less diluted the more variable the absorbance was between replicates (Figure A1). Final dilution of protein samples was around 1000 fold dilution, indicating that 0.1% of the original amount of RIPA buffer in the sample was present. This amount of buffer appeared to be safe to have present when doing the protein assay (Figure A2).

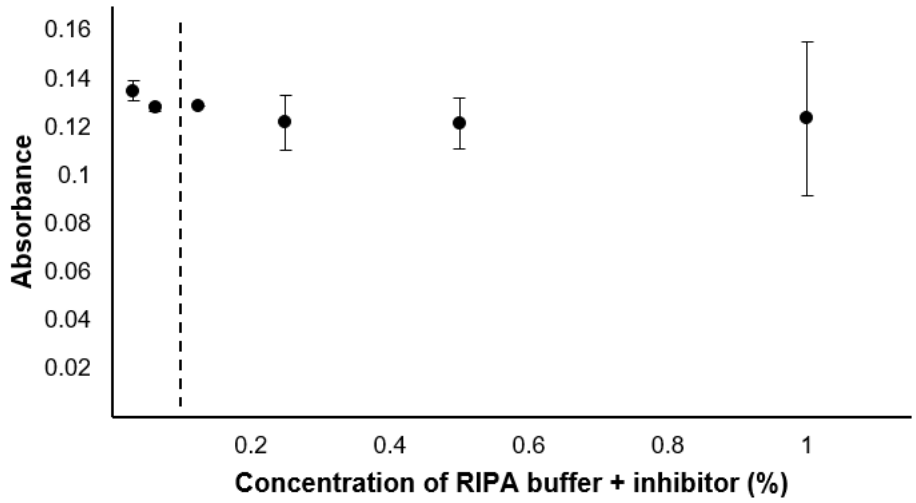

Figure A1. Bio-Rad Protein assay interference assessment with various concentrations of RIPA buffer with inhibitor (+/- 1 SD). Horizontal dash line indicates the final diluted amount of RIPA buffer and inhibitor (100% signifying no dilution) that was used for samples for the protein assay (0.1%).

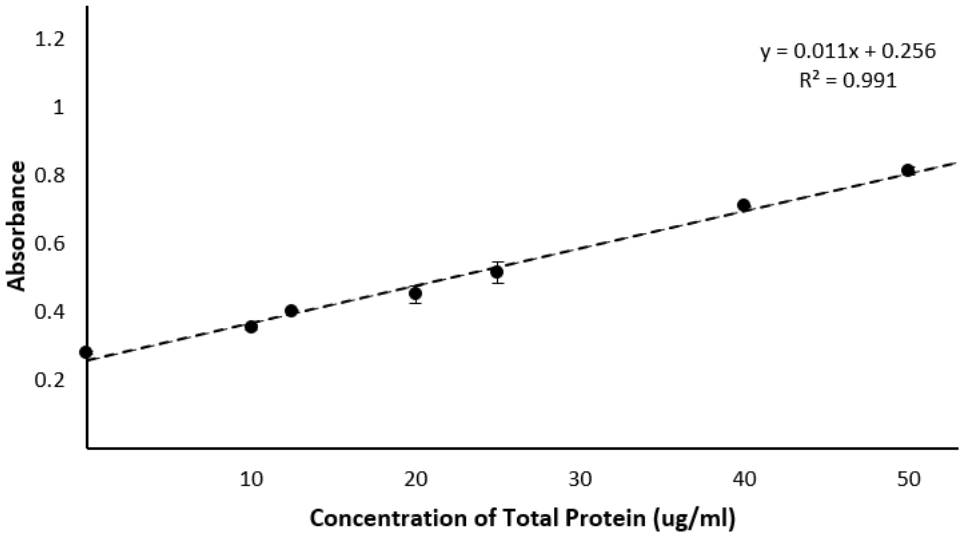

Figure A2. Bio-Rad Protein assay using Protein standard 1. Each sample was ran using triplicates (± 1 SD).

7.2 RT-qPCR

7.2.1 Annealing Temperature

The primers were manufactured to work optimally at 60 ˚C. But to ensure that they were designed appropriately, the annealing temperature was varied to compare which one was best (Figure A3). For the sake of efficiency, best annealing temperature ranges were determined and the temperature that worked for all primers was selected (Table A1). This temperature was found to be 60.6 ˚C. Note that this annealing temperature was not the singular best temperature found for each primer, but fell within a range of optimal temperatures visually selected. This value is also very close to the designed optimal temperature, which gives further validity to the design and manufacture of these primers. This initial data also indicates that each primer pair is amplifying at least one sequence within the provided samples.

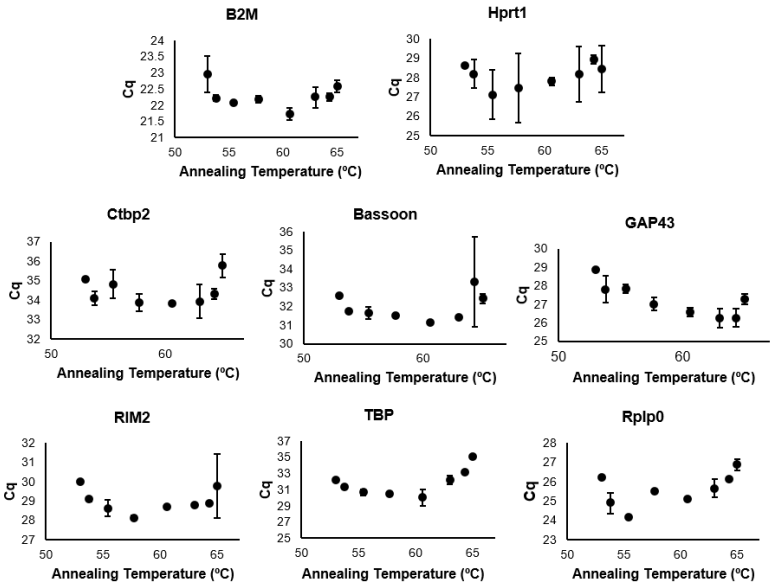

Figure A3. Annealing temperature experiment for each pair of primers to assess optimal temperature (+/- 1 SD).

Table A1. Annealing temperature experiment results for the primers.

Primer Pair	Optimal temperature range (˚C)	Chosen Annealing temperature (˚C)
B2m	53.8-64.3	60.6
Hprt1	55.4-60.6	
Ctbp2	57.7-64.3	
Bsn	57.7-63	
GAP43	60.6-64.3	
Rim2	55.4-60.6	
Tbp	57.7-60.6	
Rplp0	53.8-60.6	

7.2.2 Melt Curves

An important validity check for primers involves the assurance of their specificity when amplifying the desired cDNA sequence. When doing qPCR, the generated curve of the dye activating is a singular curve that cannot differentiate between different products.

A good primer will amplify only one product, that of the sequence of interest, allowing you to compare relative quantities between samples or groups. By applying a melt curve analysis, the number of amplified products is revealed in the number of peaks (Taylor et al., 2010). Each sample should have only one peak and all samples should resolve one peak at a similar melting temperature. For all primer pairs, a singular peak was found except for Bassoon and Rplp0 (Figure A4). However, in the case of Rplp0, this primer pair is amplifying a potential reference gene.

Interestingly, Rplp0 being a potential reference gene means that we are not interested in the specific relative quantities. All that is needed is that Rplp0 is stably expressed between the control and noise groups. Therefore, even if there are multiple products, as long as it is stably expressed, it is reasoned here that for a reference gene it is okay to have another product, which does appear to be present in all of the samples.

On the other hand, Bassoon is a gene of interest, but the melt curves show the variable presence of a second small peak, indicating a second sequence is getting amplified. However, the question is, how much of this contaminating product is present? If the concentration is low enough, then there could be potential to disregard it and use the data as is. This theory is supported by the fact that it is not in every replicate. Regardless, any relative quantity results for Bassoon are questionable due to the presence of these multiple peaks.

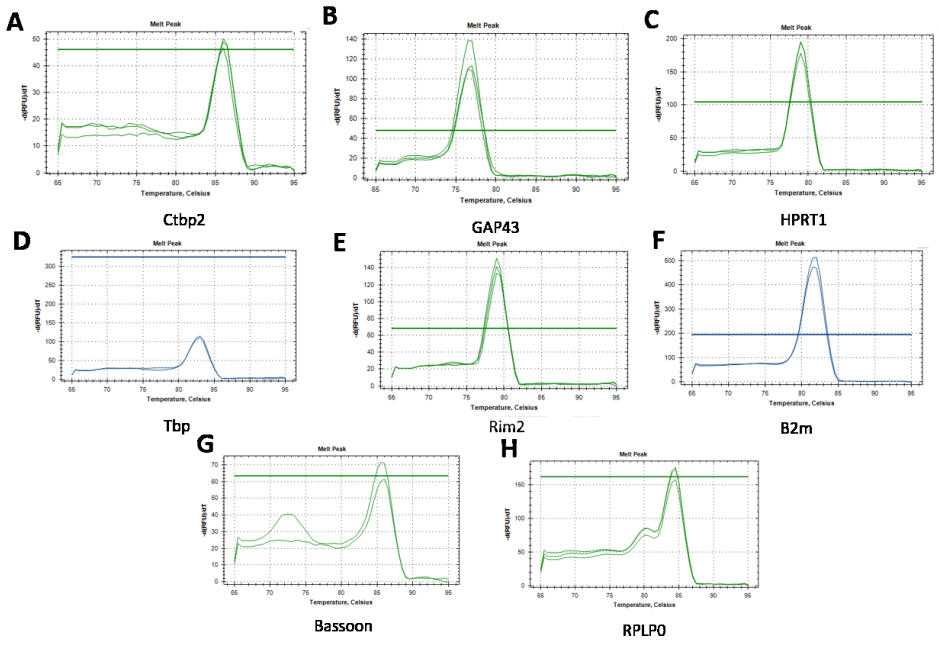

Figure A4. Melt curve experiment. Presence of a peak that does not overlap indicates more than one product, and therefore a non-specific amplifying primer. Note (G) and (H) both have multiple peaks.

7.2.3 Standard Curves

The final validity check for the primers involves determining the linear range for them (Figure A5). The two parameters that come out of this is the reaction efficiency and the linearity (r^2). The reaction efficiency is used to determine if for every reaction/cycle, the amplified product content is doubled. If this were the case for a particular pair of primers, then there would be 100% efficiency (Taylor, 2015). The ideal range of acceptable efficiencies for publication has been defined as 90-110% (Bustin et al., 2009). All primers met this criteria accept for Tbp (Table A2). Therefore, it must be excluded from further testing as a potential reference gene for this study. The linearity for B2M is also a concern by being below 0.980 which is considered a desirable cut off

value (Taylor et al., 2010). However, since the efficiency is within range, it was included for later testing.

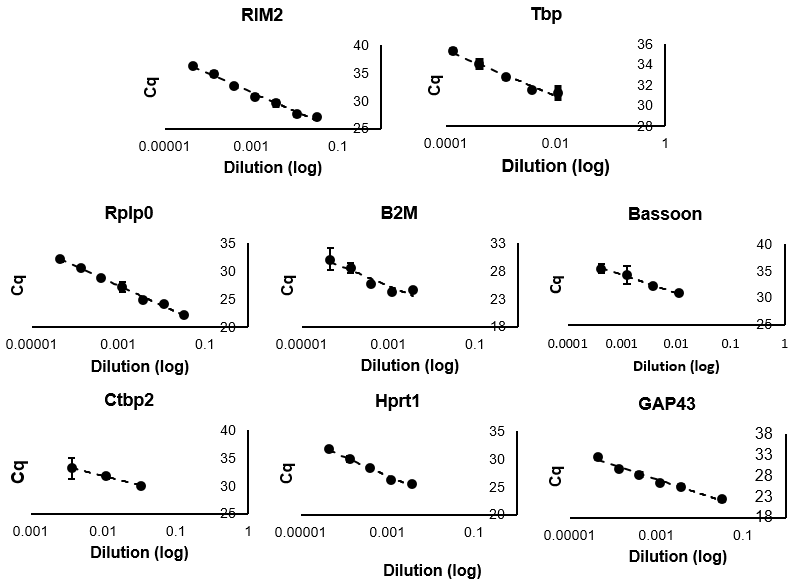

Figure A5. Standard curves of primers (+/- 1 SD).

Table A2. Efficiencies and linearity of primers' standard curve.

Primers	Efficiency (%)	r^2
Rim2	98.5	0.984
Tbp	-	0.962
Rplp0	91.9	0.993
B2M	104.8	0.879
Bassoon	97.2	0.991
Ctbp2	103.9	0.9995
Hprt1	97.2	0.981
Gap43	96.7	0.980

7.2.4 NRT/NTC Testing

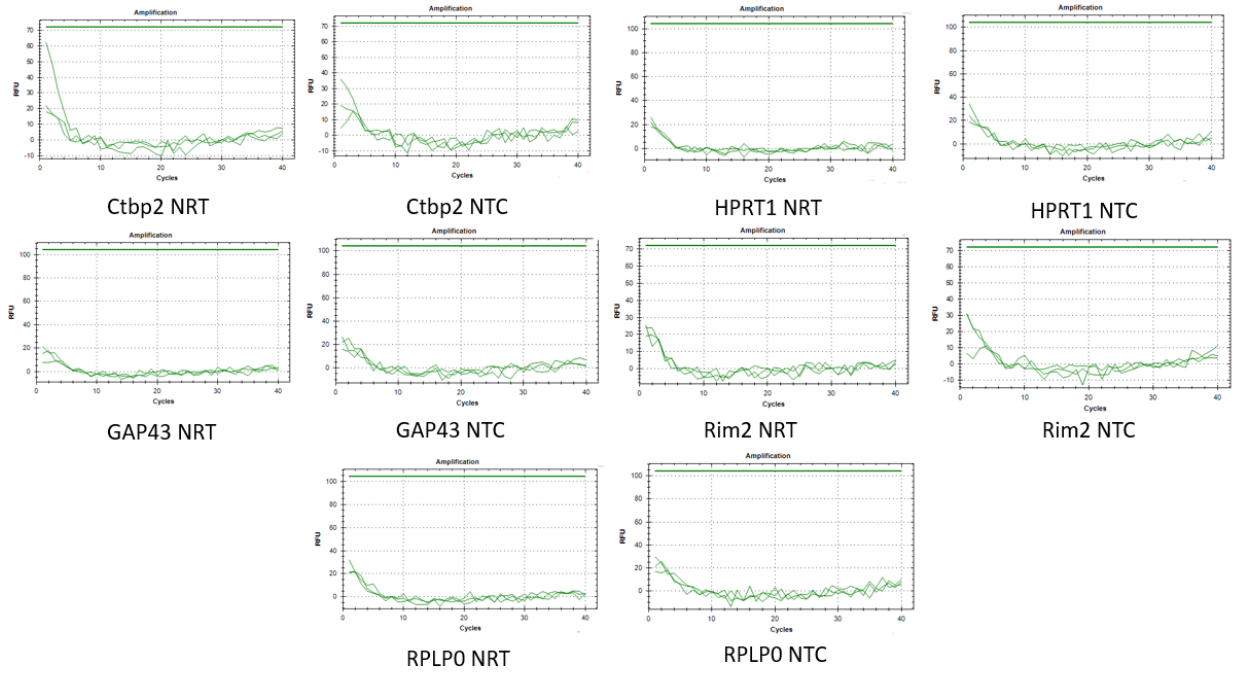

Figure A6. No-reverse transcriptase (NRT) and no-template controls (NTC) for each primer pair.